AFOSR-TR- 78-1507

ANALYSIS OF RADAR DETECTION OF AGITATED METALS (RADAM)

(12) LEVEL II

Final Report

September 1978

By: A. J. Bahr, V. R. Frank, J. P. Petro,
L. E. Sweeney, Jr., and O. G. Villard, Jr.

Prepared for:

Air Force Office of Scientific Research
Directorate of Electronic and
Solid State Sciences
Bolling Air Force Base, Building 410
Washington, D.C. 20332

Attention: Dr. George E. Knausenberger
Program Manager, AFOSR/NE

Contract F44620-75-C-0046

SRI International
333 Ravenswood Avenue
Menlo Park, California 94025
(415) 326-6200
Cable: SRI INTL MNP
TWX: 910-373-1246

The research reported herein was sponsored by the Air Force Office of Scientific Research (AFSC), United States Air Force, under Contract F44620-75-C-0046. The United States Government is authorized to reproduce and distribute reprints for governmental purposes notwithstanding any copyright notation hereon.

SRI International

(6) # ANALYSIS OF RADAR DETECTION OF AGITATED METALS (RADAM).

(9) Final Report
1 Apr 77 to 15 Jul 78

(11) September 1978

(12) 61 p.

(10) A. J. Bahr, V. R. Frank, J. P. Petro, L. E. Sweeney, Jr., O. G. Villard, Jr.

(18) AFOSR

Prepared for:

Air Force Office of Scientific Research
Directorate of Electronic and Solid State Sciences
Bolling Air Force Base, Building 410
Washington, D.C. 20332

(19) TR-78-1507

Attention: Dr. George E. Knausenberger
Program Manager, AFOSR/NE

(15) Contract F44620-75-C-0046

(16) 2305

(17) B2

SRI Project 4176

Approved for Public Release; Distribution Unlimited.

Approved by:

Lawrence E. Sweeney, Director
Remote Measurements Laboratory

David A. Johnson, Executive Director
Technology and Systems Development Division

Copy No. 15

410 281

CONTENTS

ILLUSTRATIONS

ACKNOWLEDGMENTS

It has been both stimulating and gratifying to receive the enthusiastic support of Dr. G. E. Knausenberger of AFOSR during this research program. The additional support for field measurements received from Mr. M. Shirazi of the Air Force Avionics Laboratory played a key role in the success of this program. Many other people contributed to stimulating and helpful discussions during this program, especially Dr. R. B. Mack, formerly of the RADC Deputy for Electronic Technology, Professor A. A. Ksienski of Ohio State University, and Mr. J. R. Nichols of the Naval Weapons Center. Messrs. C. A. Cole, R. E. Wanner, K. E. Johansen, C. P. Powell, A. G. Tomlin, W. B. Weir, and D. D. Lee, all of SRI, also contributed significantly to the program.

I. INTRODUCTION

It has been observed that the radar returns from moving multi-element metal targets often exhibit an unexpected modulation that has both random (or noise-like) and semicoherent components. This modulation might be produced by modification of the current distribution on the target that results when electrical contacts between target elements are altered intermittently by the forces associated with target motion. This intermittent-contact modulation must be considered when designing a radar for detecting or identifying a target exhibiting this effect. Depending on the application, the observer may wish to enhance or suppress the observation of the effect, or it may be important that the effect itself be enhanced or suppressed. To accomplish any of these, the effect must be well understood. Therefore a research program was undertaken at SRI to study the intermittent contact aspect of the radar detection of agitated metals (RADAM). This report summarizes the results of that program.

The overall objectives of the RADAM research program were to (1) identify and isolate the physical processes and mechanisms that contribute to a RADAM signature, (2) identify and explain important recognizable features of the signature, and (3) determine means for separating the meaningful identifying components of the signature from nonmeaningful ones. All these objectives have been achieved by combining the results of laboratory experiments using simple scatterers, electromagnetic scattering theory, and field experiments using complex targets such as a tank. A model for the intermittent-contact RADAM effect (hereafter simply called RADAM) has been proposed. This model and the experimental evidence to support it are reviewed in Section II. Section III discusses the distinctive features and the physical interpretation of the RADAM signature for a tracked vehicle. Experiments aimed at explaining the physical source of RADAM in tracked vehicles were carried out using a scale model; the results and conclusions of this work are presented in

Section IV. In Section V, a real-time digital target-identification processor for RADAM signals is described and some examples of processed VHF backscattering data obtained from some tracked vehicles are presented. Section VI contains the conclusions and recommendations derived from this work.

To date, the following publications have resulted from this work:

- V. R. Frank, J. P. Petro, and A. J. Bahr, "Backscattering from a Cylindrical Dipole Centrally Loaded by a Time-Varying Impedance," IEEE Trans. on Antennas and Propagation, Vol. AP-25, pp. 356-358 (May 1977).
- A. J. Bahr, V. R. Frank, J. P. Petro, and L. E. Sweeney, Jr., "Radar Scattering from Intermittently Contacting Metal Targets," IEEE Trans. on Antennas and Propagation, Vol. AP-25, pp. 512-518 (July 1977).
- A. J. Bahr and J. P. Petro, "Experimental Comparison Between Induced Surface Current and Scattered Electromagnetic Waves for a Metal Target with Time-Varying Characteristics," Electronics Letters, Vol. 13, pp. 777-778 (December 1977).
- A. J. Bahr and J. P. Petro, "On the RF Frequency Dependence of the Scattered Spectral Energy Produced by Intermittent Contacts Among Elements of a Target," IEEE Trans. on Antennas and Propagation, Vol. AP-26, pp. 618-621 (July 1978).

II. LOADED-SCATTERER MODEL FOR INTERMITTENT-CONTACT RADAM

In general, several physical mechanisms can cause modulation of the radar scattering from a moving multielement metal target. Modulation can occur if the aspect of the target relative to either the transmitting or receiving antennas changes, and Doppler effects (phase modulation) can be produced by motion of the target as a whole or by the relative motion of target elements. In addition, the scattering will change if the surface currents on the target are modified by intermittent changes in the electrical contact between different target elements;[1*] this effect is called intermittent-contact RADAM, or simply RADAM. The use of RADAM signatures for target identification appears attractive because the RADAM modulation comprises relatively rapid variations, and thus the RADAM modulation can be separated rather easily from the other types of modulation and from background clutter. Furthermore, the RADAM signatures appear to be related to physical characteristics of the target. The loaded-scatterer model described in this section is useful for explaining the observed characteristics of RADAM modulation.

The term "loaded scatterer" refers to a scatterer with one or more pairs of local terminals (ports) to which an electrical impedance or impedances are connected.[2,3] The scattering thus becomes a function of these impedances. If a scatterer has two or more separate parts that intermittently make contact, one can consider the points of contact to be a pair of terminals. The impedance connected to these terminals is then either essentially a short circuit (the RF contact impedance between two metal surfaces is usually small even for point contacts) or essentially a capacitive reactance. The latter situation occurs if the contact is open or if there is an oxide or other nonconducting substance on the surface.

---

*References are listed at the end of this report.

In this model, then, the observed changes in scattering are considered to result from changes in the contact impedance of the various contacts on the scatterer. For this model to be valid, changes in impedance must take place slowly enough, so quasi-steady-state conditions prevail. A "slow" enough variation is longer than the transient response of the target. This condition is satisfied for most practical cases.

A very simple, but general, expression for the received component of the scattered electric field, E^S, as an explicit function of load impedance, Z_L, can be written for a target having a single loading port.[3,4] This expression is:

$$E^S(Z_L) = E^S(Z_0) \left[1 - \alpha\left(\frac{Z_L - Z_0}{Z_L + Z_r}\right)\right] \qquad (1)$$

where Z_0 is a reference impedance (for example, zero for a short circuit), Z_r is the radiation impedance of the target if it were driven by a generator connected to the load terminals, and α is a complex coupling factor that depends on the radar parameters and on the target geometry. Physically, α is a measure of the coupling between the surface currents on the target and the load impedance.

Suppose that Z_0 is zero, i.e., that the reference condition corresponds to the case where the two metal elements of the target are in contact. From Eq. (1), the conditions for obtaining a large degree of modulation are (1) that the contact be located where the surface currents are relatively large and produce scattering in the direction of the receiver, and (2) that Z_L vary between zero and a number large compared with Z_r.

This model has been verified for a dipole (simple scatterer).[5,6] Measurements were made of the backscatter from a bisected dipole of 17.8-cm total length that was made of 0.159-cm diameter brass welding rod. The dipole was cut in the middle at a 45° angle, and the resulting surfaces were sanded smooth. The dipole halves were mounted under elastic tension; by pulling on a string attached to one side of the dipole, the contact surfaces could be periodically separated by 1 to 2 mm.

One experiment was conducted at the resonant frequency of the dipole--825 MHz. Figure 1 shows the measured backscatter signal as a function of time. There is a large change in radar cross section, $\Delta\sigma$, between open and closed states. In terms of Eq. (1), α is large because the contacts are at the center of the dipole where the current is largest (particularly at resonance), Z_0 is zero, Z_r is real, and Z_L varies between zero and a capacitive reactance. All these conditions lead to a large change in radar cross section, and the experimental value of this change was found to agree[6] with that calculated from the theory of Hu.[7] Note that the backscattering changes very rapidly after the contact is made or broken.

The backscattering behaves differently at other frequencies. For example, the experimental results obtained with the same dipole at a frequency above resonance are shown in Figure 2. The frequency was chosen so that the steady-state backscattering would be the same in both the open and closed states. However, it can be seen that a change in backscattering occurs during the transition between these two states. For example, as the contact starts to close, the backscattering begins to increase. This increase can be interpreted as being caused by the variable "tuning" of the inductive reactance of the above-resonance dipole by the changing capacitive reactance of the contact; as soon as metallic contact is made, the backscattering drops to its steady-state value. Just the reverse takes place when the contact opens. Similar behavior will occur at other frequencies above resonance, but the steady-state backscattering for the open and closed states will be different. It will be seen later that the backscattering from tracked vehicles exhibits very similar time-domain behavior in the VHF range: a "slow" variation in backscatter is followed by a very fast change, and vice versa. This time-domain behavior appears to be a distinguishing characteristic of RADAM, and it can be used as a basis for constructing RADAM signatures.

Equation (1), the loaded-scatterer model, can thus be used to predict the magnitude and frequency dependence of the backscatter modulation produced by a varying load impedance. This has been calculated for

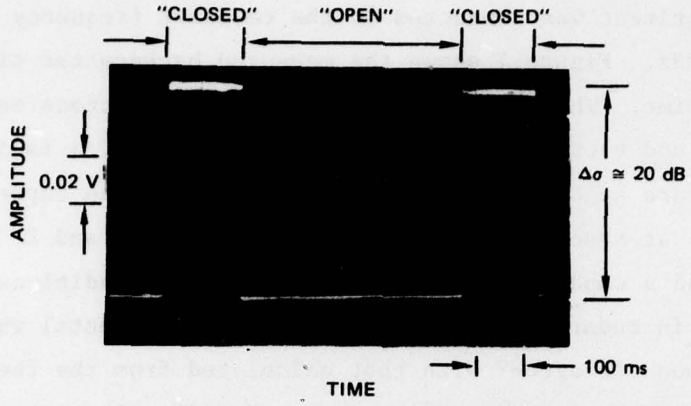

FIGURE 1 MEASURED BACKSCATTERED SIGNAL FROM 17.8-cm LONG MECHANICALLY SWITCHED DIPOLE AT 825 MHz

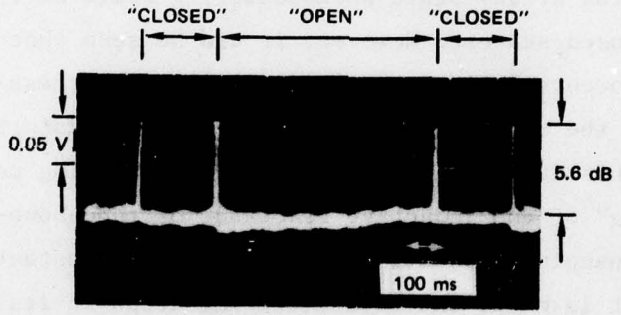

(a) AMPLITUDE vs TIME

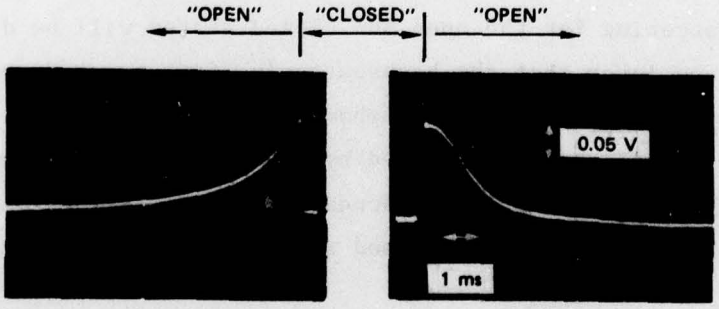

(b) AMPLITUDE vs TIME, EXPANDED TIME SCALE

FIGURE 2 MEASURED BACKSCATTERED SIGNAL FROM 17.8-cm LONG MECHANICALLY SWITCHED DIPOLE AT 1010 MHz.

a dipole,[4] but it is much more difficult to do for more complex scatterers. Nevertheless, the theoretic and experimental results obtained for a dipole have proved very useful for understanding the experimentally observed scattering characteristics for a complex target like a tracked vehicle. These tracked-vehicle scattering characteristics and their interpretation are discussed in the next section.

III. CHARACTERISTICS OF VHF RADAM FROM TRACKED VEHICLES

A. Field Experiments

From May 1976 through September 1977, supplementary support was received from the Air Force Avionics Laboratory, RWM-6, to expand the experimental part of this program to include field measurements of the VHF scattering from tactical vehicles. The vehicles studied were two tracked vehicles--a tank and an armored personnel carrier (APC)--and a truck.

The scattering measurements for these targets were carried out using a continuous-wave (CW) radar with provisions for nulling the clutter detected in the absence of a target. The layout of the radar range and vehicle course is shown in Figure 3. The bistatic angle for this radar was about 36 degrees. The data were taken as functions of frequency, aspect angle, polarization, and vehicle speed and then processed and analyzed in both the time and frequency domains.[8]

B. Modulation Characteristics

The major result of these field experiments was the discovery of large modulations on the scattering from the tracked vehicles. Typical backscatter waveforms and spectra for a tank and an APC are shown in Figures 4 and 5, respectively. The time-domain waveforms show large amplitude (up to 50% index of modulation) and phase modulation for both types of vehicles. These modulations resemble rectangular pulses and occur at irregular intervals. The RADAM "pulses" rise and fall relatively rapidly. The aperiodic nature of the modulation is evident in the spectra, where it can be seen that the spectral energy associated with the modulation is spread over a wide frequency range. Hence the energy contained in any particular narrow spectral range is usually not large enough to be used for target identification. On the other hand, the large degree of modulation and its distinctive character in the

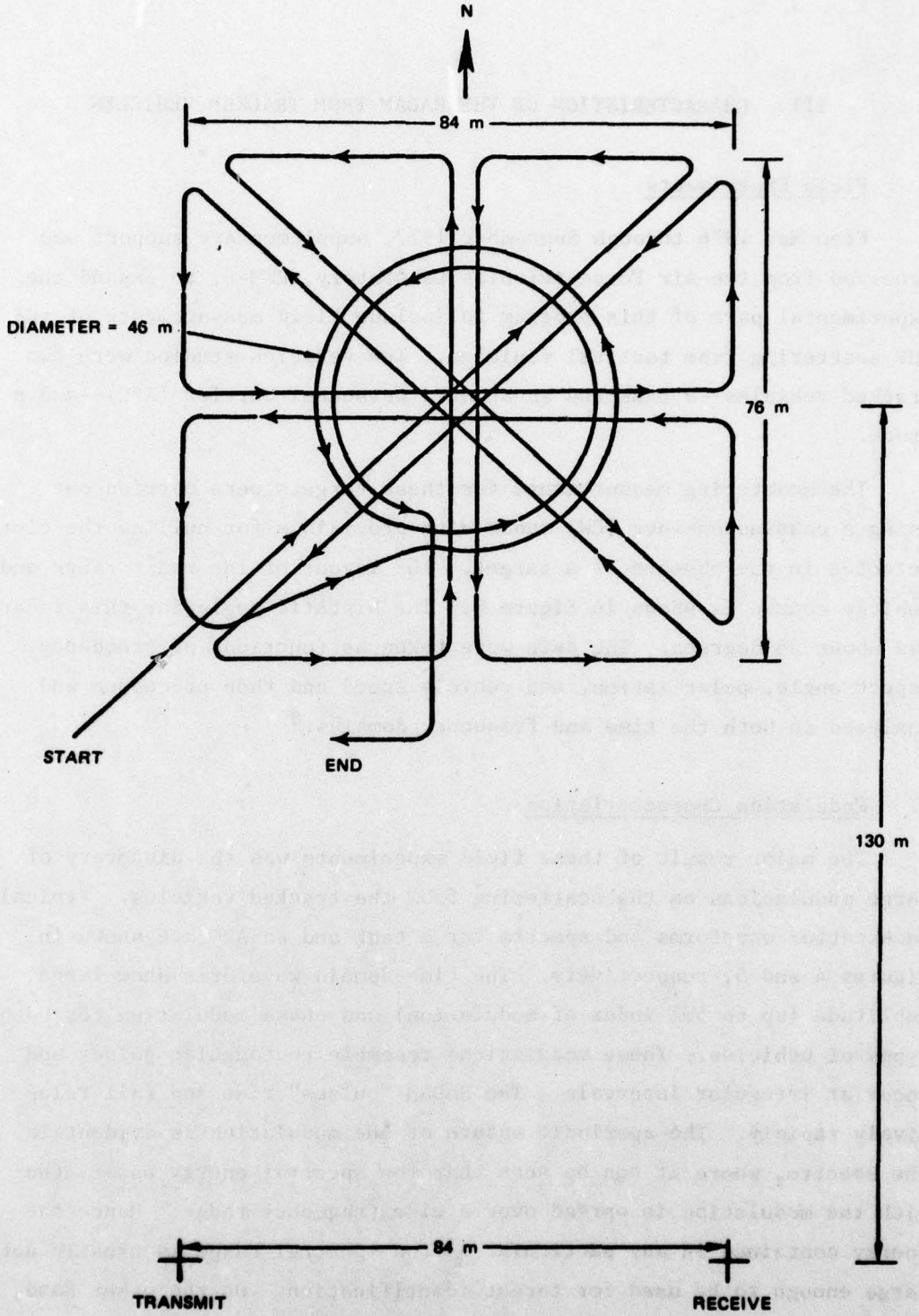

FIGURE 3 LAYOUT OF COURSE TRAVERSED BY VEHICLES DURING RADAM FIELD TESTS

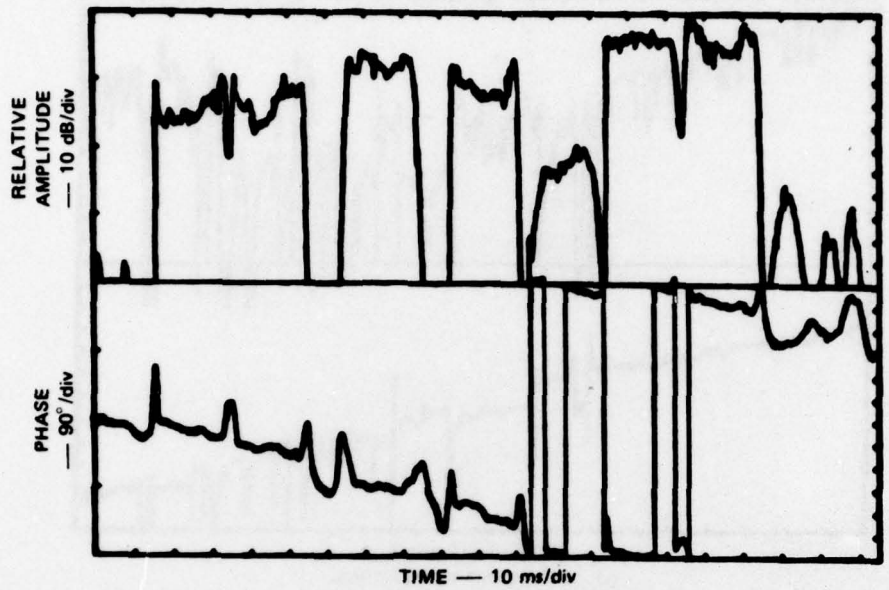

(a) DETECTED WAVEFORMS

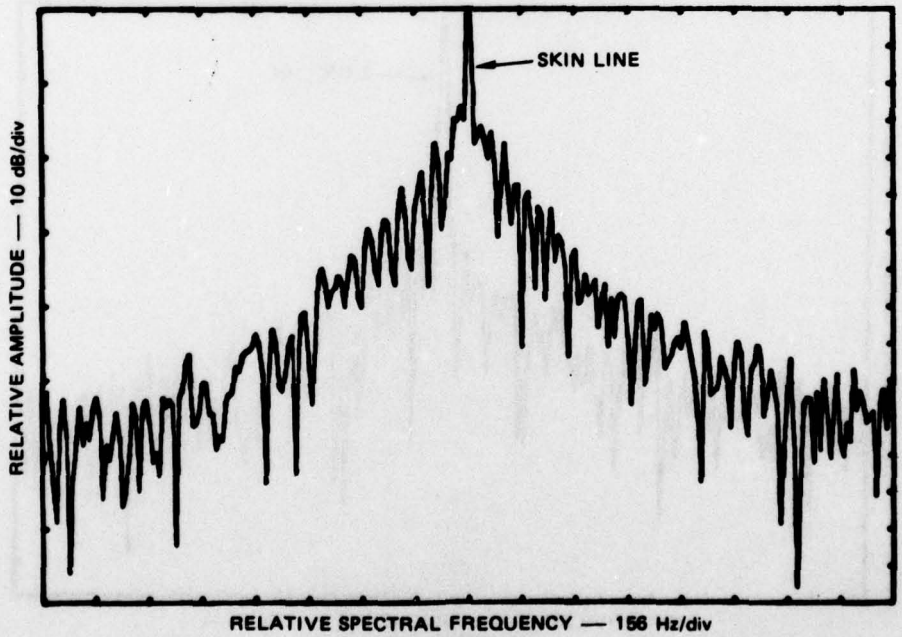

(b) SPECTRUM

Speed: 15 mph
Polarization: Vertical
Aspect: 225°

FIGURE 4 VHF BACKSCATTER WAVEFORMS AND SPECTRUM FOR A TANK

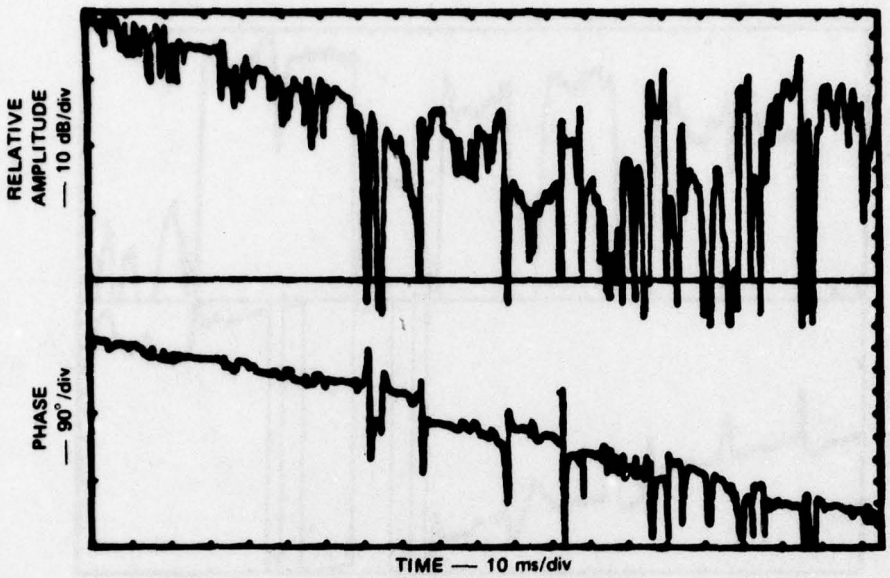

(a) DETECTED WAVEFORMS

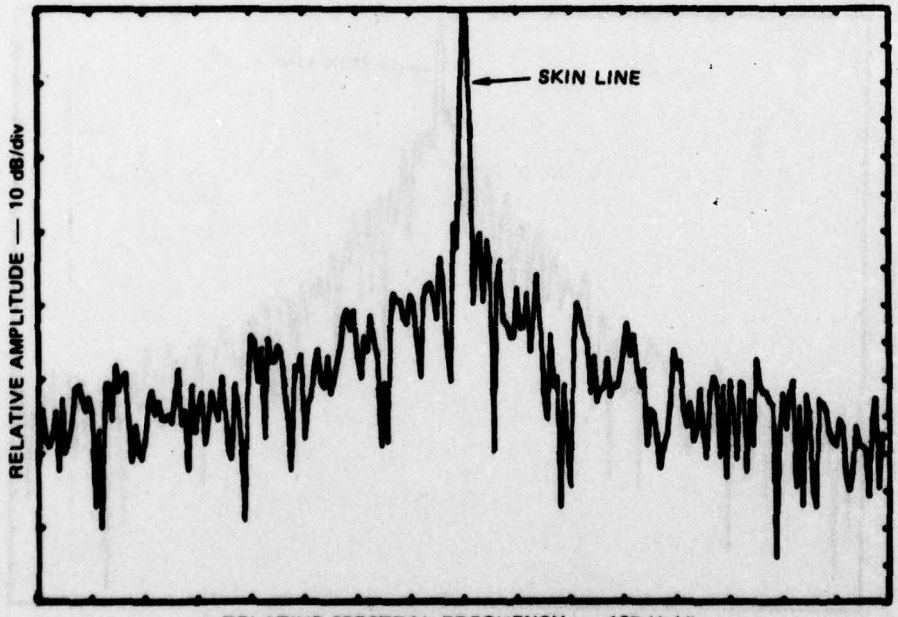

(b) SPECTRUM

Speed: 15 mph
Polarization: Vertical
Aspect: 225°

FIGURE 5 VHF BACKSCATTER WAVEFORMS AND SPECTRUM FOR AN APC

time domain suggest that some form of time-domain processing might lead to a practical means for identifying tracked vehicles. The truck produced relatively little of this type of modulation.

Figures 6 and 7 illustrate the distinctive time-domain behavior of the amplitude modulation on the VHF backscatter from a tank and an APC, respectively, in more detail. The observed modulation is seen as rapid changes in amplitude that occur within 1 to 2 ms, plus some slower variations in amplitude. In general, if the amplitude increases rapidly at a particular instant, the next rapid change will usually be a decrease in amplitude, and vice versa. Thus, the RADAM modulation takes on the general appearance of a series of square-topped "pulses."

Close examination of these pulse-like waveforms shows that their distinguishing feature is the temporal behavior near a pulse edge. Each pulse edge can be characterized as a rapid change in amplitude followed by a slower change, or vice versa. This behavior is similar to that observed for a mechanically switched dipole (Figures 1 and 2); it suggests that a single contact on the vehicle is responsible for the modulation. Assuming this model to be correct, one can identify time periods in the waveforms that correspond to the contact being "open" and "closed." According to this interpretation, then, the RADAM pulse shown in Figure 6 occurs when the contact is closed, while those shown in Figure 7 occur when the contact is open. Of course, this conclusion depends on the definition of a RADAM pulse.

For example, suppose a RADAM pulse duration is defined as the time during which the contact is closed. Then the start of a RADAM pulse would be characterized by a slow variation followed by a fast variation, and the end of a RADAM pulse would be defined by the opposite sequence. With this simple algorithm, the beginning and end of a RADAM pulse can be defined, and timing circuitry can be used to measure such pulse characteristics as the duration or the pulse interval.

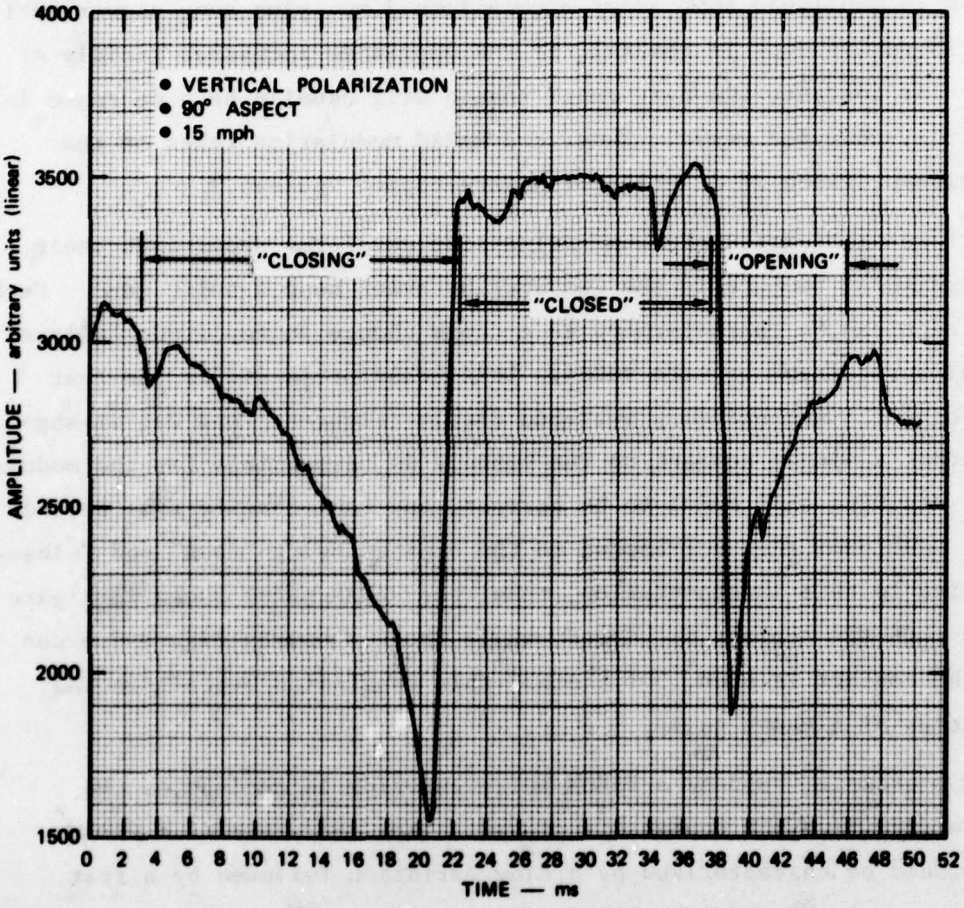

FIGURE 6 DETAILED TIME-DOMAIN BEHAVIOR OF VHF BACKSCATTER FROM A TANK

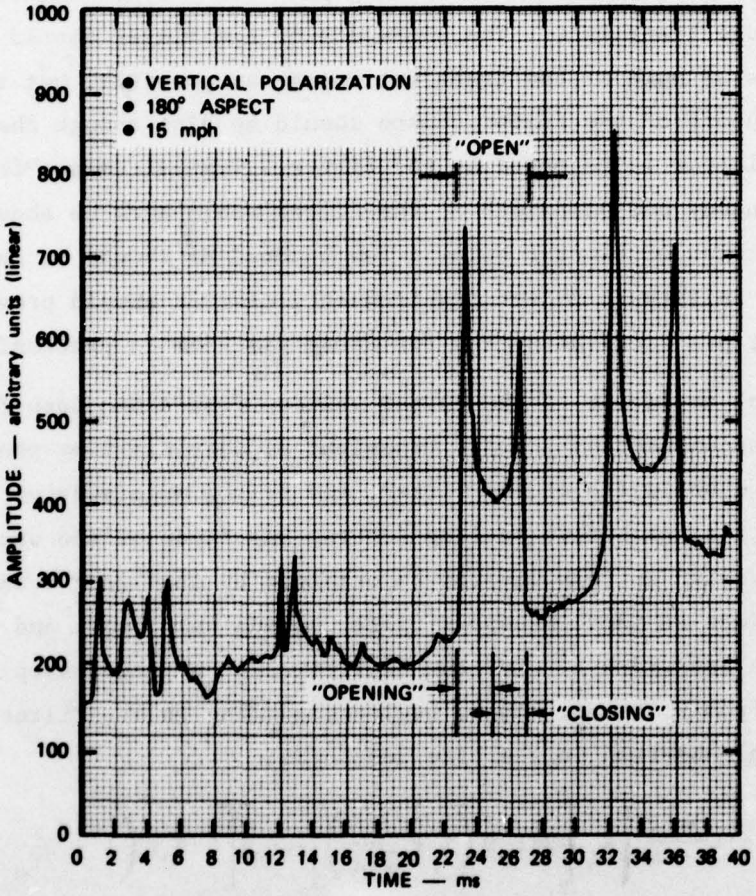

FIGURE 7 DETAILED TIME-DOMAIN BEHAVIOR OF VHF BACKSCATTER FROM AN APC

C. Effect of Bandpass Filtering

Timing pulses that establish the beginning and end of a RADAM pulse can be generated from the detected amplitude-modulated signal by passing it through a bandpass filter. The chosen center frequency of the filter should be equal to the reciprocal of the average of the rise and fall times of the RADAM pulse to efficiently pass the energy associated with the pulse-edge transients. The bandwidth of the filter should be large to encompass as much of the transient energy as possible, but the low-frequency cutoff of the filter chosen should be high enough that low-frequency clutter is rejected by the filter. Typical values for the center frequency and bandwidth of the filter would each be about 1 kHz, so the rejection of clutter below a few hundred Hz should be relatively easy. This ability to reject low-frequency clutter should prove to be an important practical advantage for RADAM time-domain processing.

The peak amplitude of the output voltage from a bandpass filter that has been excited by a sharp transient is determined by the center frequency and bandwidth of the filter, and by the magnitude of the transient. A quantitative feeling for the magnitude of the output voltage generated in this way can be obtained by analyzing a simple case. Consider an ideal bandpass filter having unity gain and centered at f_0 with a bandwidth B. Let the excitation be a single step function in voltage from V_1 to V_2. Then, neglecting delay in the filter, the output signal observed in the time domain is:

$$\frac{V_{out}}{V_1} = \frac{1}{\pi} \frac{2m}{1+m} \left\{ S_i \left[2\pi f_0 t \left(1 + \frac{B}{2f_0} \right) \right] - S_i \left[2\pi f_0 t \left(1 - \frac{B}{2f_0} \right) \right] \right\} \quad (2)$$

where

$$S_i(z) = \int_0^z \frac{\sin x}{x} \, dx \quad (3)$$

and

$$m = \frac{V_1 - V_2}{V_1 + V_2} \quad . \tag{4}$$

Equation (2) describes a decaying sinusoid-like waveform. For example, if $B = f_0$, the peak value of the difference of sine integrals in braces is nearly unity and occurs at approximately $2\pi f_0 t = \pi/2$. Hence

$$\left.\frac{V_{out}}{V_1}\right|_{peak} \simeq \frac{1}{\pi}\,\frac{2m}{1+m} \quad . \tag{5}$$

It can be seen that V_{out}/V_1 is relatively large if the modulation index, m, is large. Clutter frequencies of less than $f_0/2$ are rejected by the filter.

Experimental results obtained using an active filter with a 3-dB bandwidth of 1 kHz centered at 1 kHz are shown in Figure 8. In Figure 8(a), the upper trace is the detected amplitude waveform obtained for a tank, and the lower trace is the corresponding output of the bandpass filter. Figure 8(b) shows the results obtained when the cross section of the tank was nearly the same for the open and closed states. The RADAM pulses are no longer square-wave in character but are defined by pairs of impulses. For either type of RADAM waveform, the short pulses emerging from the filter are always bipolar, and the magnitude of the polarity corresponding to the slower change in backscatter amplitude is always less than that of the other polarity. Thus, by comparing the magnitudes of the two polarities, one can always tell whether the contact is closing or opening. For a closing contact the first half of the corresponding bipolar pulse is smaller than the second half. The reverse is true for an opening contact. This comparison forms the basis of an algorithm for determining the beginning and end of a RADAM pulse.

(a) "SQUARE-WAVE" RADAM

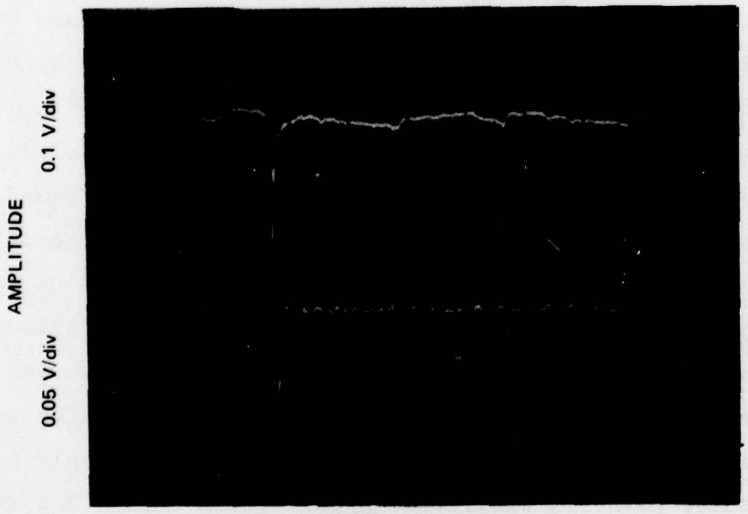

(b) "IMPULSIVE" RADAM

FIGURE 8 COMPARISON OF OUTPUT WAVEFORMS FOR THE AMPLITUDE DETECTOR AND BANDPASS FILTER

IV. EXPERIMENTAL STUDIES OF A SCALE-MODEL TRACKED VEHICLE

A. Description of Experiment

The observance of the large modulation on the VHF scattering from full-scale tracked vehicles, and the similarity of these waveforms to those produced in the laboratory by single contacts was somewhat surprising in view of the complex nature of a tracked vehicle. Therefore it was important to try to identify the source of this modulation and to learn more about the dependence of the modulation on frequency, aspect angle, and polarization. Since the cost of using full-scale tracked vehicles is prohibitive, a 5:1 reduced-scale model of a tank was constructed and exploratory tests using this model were carried out in the laboratory.

A photograph of the scale-model tank is shown in Figure 9. For simplicity, the model had only the general shape of a tank and only one track. The nominal dimensions of the model were 4 ft (1.89 m) long, 1.5 ft (0.71 m) wide, and 1.25 ft (0.59 m) high. The track was constructed from a chain-driven conveyor belt that had "tread" plates 1.4 in (3.56 cm) wide and 4.4 in (11.18 cm) long. The drive chain for the conveyor belt was attached to the middle of the tread plates [Figure 9(b)]. This method of drive differs somewhat from the method used in an actual tank, where the drive is applied at each end of the treads by dual sprockets.

The motor for driving the track on the model was within the copper-screen-covered tank body. Thus the only moving metal-to-metal contact exposed to the radar was that between the metal sprocket and the drive chain (the idler wheels were nonmetallic). The model shown in Figure 9 simulates a situation in which the cannon is in the stowed position, which was the case for the full-scale tank used in the field experiments; the forward direction of travel is such that the cannon is in the rear (the track in the figure moves clockwise).

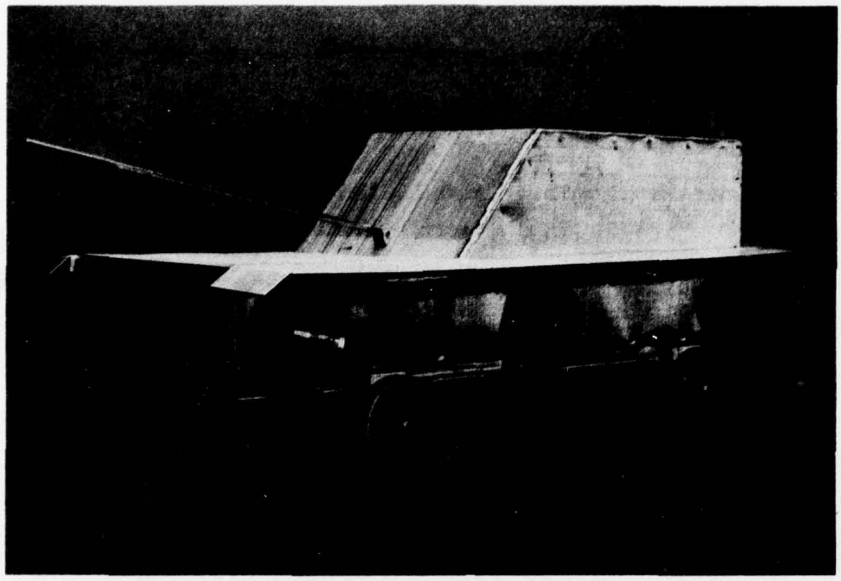

(a) FULL VIEW

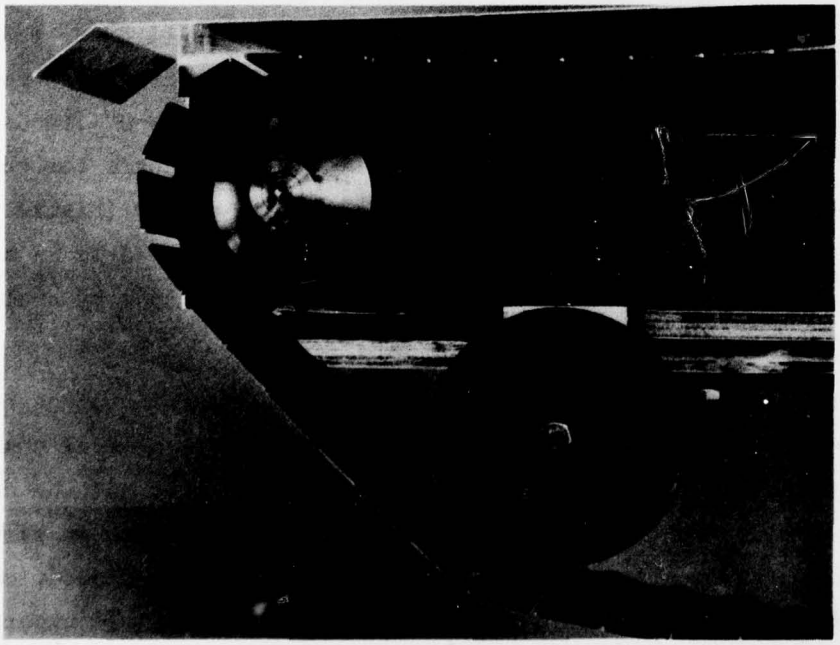

(b) DETAILED VIEW OF SPROCKET AND CHAIN

FIGURE 9 SCALE-MODEL TANK

The measurements were made on a rooftop range, whose layout is shown in Figure 10. The bistatic angle for this range was about 20 degrees (compared with 36 degrees in the field experiments). The model was raised about 6 ft (2.0 m) and the antennas about 7 ft (2.13 m) above the roof. The model was mounted on a pedestal so that it could be turned to vary its aspect angle relative to the radar. The antennas were wideband rectangular-aperture horns that could be operated over a frequency range of 500 to 2000 MHz. The linearly polarized horns were rotated about their beam axes to orient the polarization either vertically or horizontally. The antenna apertures were small enough that the target was always well within the far fields of the antennas at the measurement frequencies.

A computer-controlled Hewlett-Packard 8542B automatic network analyzer (ANA) was used for the transmitter and receiver in this system. The available CW power provided by the ANA at the transmitting antenna after amplification ranged from 80 mW at 500 MHz to 5 mW at 1100 MHz. This system also incorporated a digitally controlled nulling network that permitted the range to be automatically nulled at each frequency, which greatly facilitated making the scattering measurements at many discrete frequencies over a broad frequency range.

The measurement procedure was as follows. First, the range was nulled at a prescribed set of frequencies either without the model in place, or with it in place without its motor running. The corresponding nulling network parameters for each frequency were automatically stored in computer memory. Typical isolations achieved between the transmitting and receiving antennas were between 60 and 80 dB, depending largely on the amount of wind present (there were some trees in the field of view of the radar). Second, the model was placed in the range and its motor was turned on. Then scattering measurements were taken at frequencies between 550 and 1050 MHz, with each specific frequency being determined by the computer. The computer also set the nulling network at each frequency in accordance with the results of the nulling measurements. The demodulated amplitude and phase of the scattered signal were derived from the ANA outputs and recorded on analog tape in an FM format at 60 ips. The video bandwidth of the amplitude signal at the tape recorder

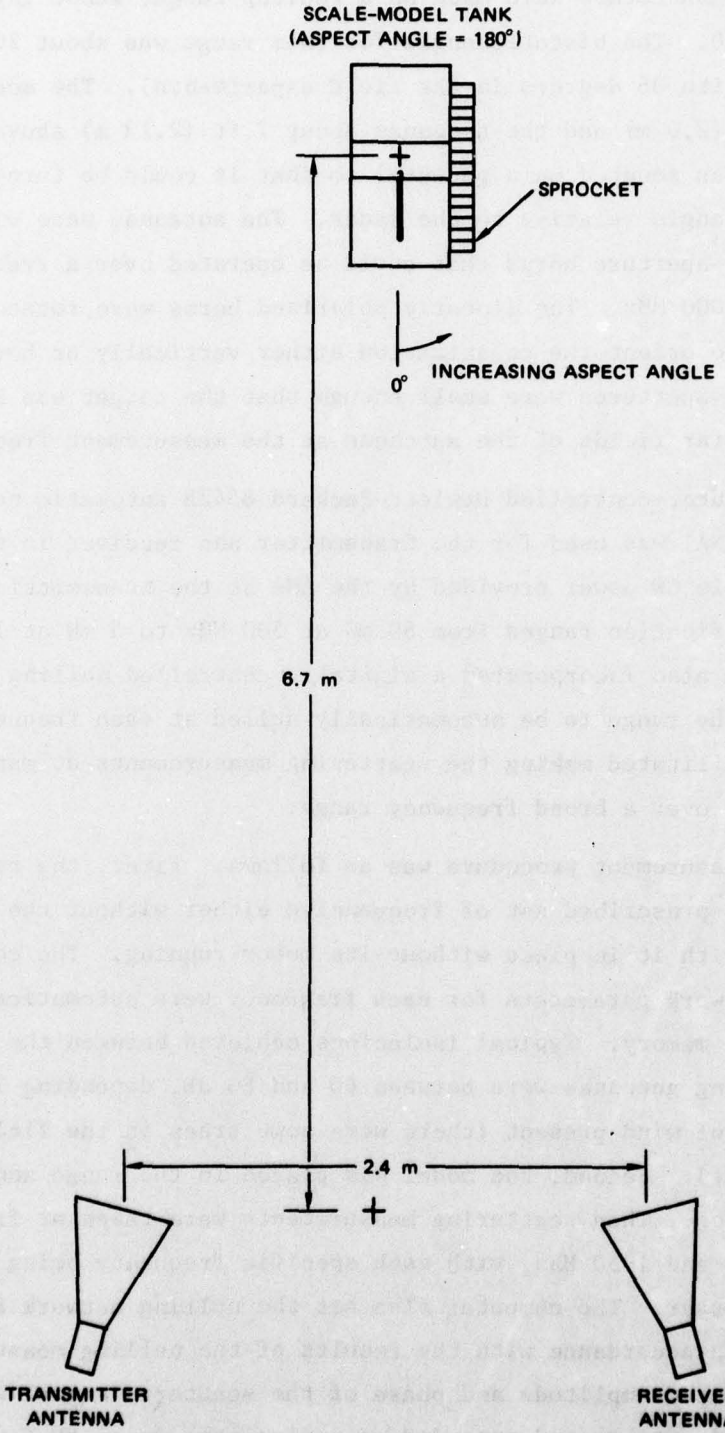

FIGURE 10 LAYOUT OF ROOF-TOP RANGE

input was 5 kHz; the video bandwidth of the phase signal was 10 kHz. The bandwidth of the tape recorder at 60 ips was 10 kHz.

Only relative measurements were taken, since the objective was to look for variations produced by changes in frequency, polarization, aspect, and type and location of contact. Thus no range calibration was required.

Typically, data were recorded for about 10 seconds for each experimental condition. The data were displayed by playing back the tape at 1-7/8 ips into a chart recorder. Chart speeds of 10 to 100 mm/s were used, resulting in time-scale resolutions of between 3 and 30 ms/cm. The corresponding display bandwidth was estimated to be about 2 kHz.

B. Experimental Results

Preliminary experiments revealed that the model produced a large modulation of the scattering at certain frequencies and aspect angles. Hence, to study the frequency dependence of the scattering, the model was oriented at the aspect angle that produced the largest modulation (45 degrees), and data were taken at various frequencies. The amplitude and phase of the scattering as functions of time are shown in Figure 11. The polarization for both transmitting and receiving antennas was vertical in this case. The modulation did not become large until the frequency exceeded about 700 MHz. When one takes the scale factor of the model into account, one finds that this result agrees generally with the results obtained in the full-scale field experiments.[8] It can also be seen in Figure 11 that the modulation does not noticeably diminish at the highest frequencies used. Unfortunately, the frequency limitations of the measurement system did not permit the high-frequency roll-off characteristics of the modulation to be studied. One can detect, however, a "smoothing" of the modulation as frequency is increased, indicating that capacitive effects in the contact begin to dominate at high frequencies.

The general features of the modulation observed were periodic with time, as would be expected since the only forces on the track were those

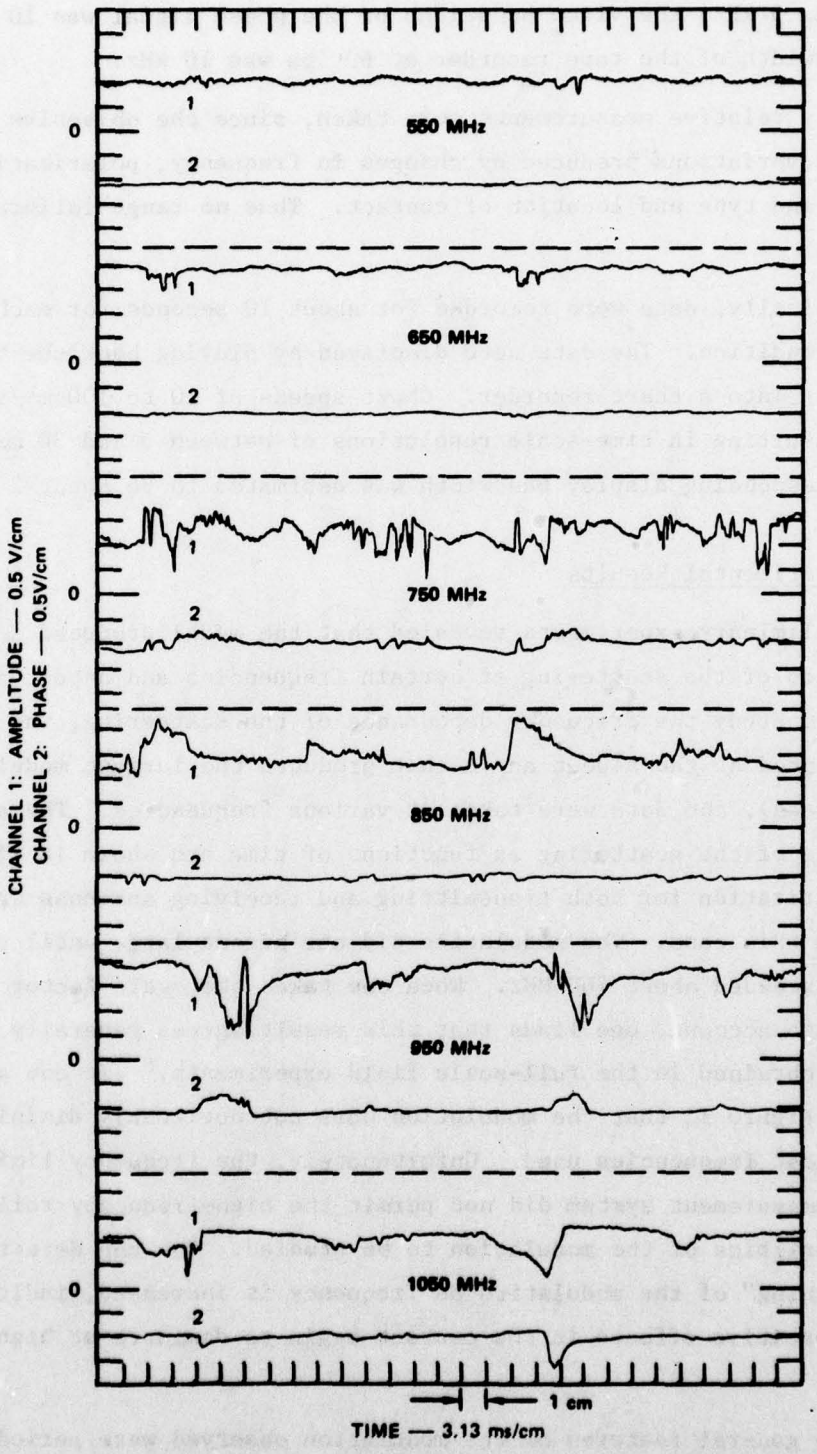

FIGURE 11 SCATTERING AMPLITUDE AND PHASE VERSUS TIME AND FREQUENCY FOR MODEL TANK (Vertical Polarization, 45° Aspect)

of the motor and gravity. The period obtained from Figure 11 is 24 ms. Since the sprocket was revolving at 225 rpm and 11 different treads engage the sprocket during one sprocket revolution, 24 ms is the time required for the track to move the distance between treads.

The same experiment was repeated using horizontally polarized transmitting and receiving antennas; the results are shown in Figure 12. The modulation in this case was considerably smaller than that obtained with vertical polarization and is only noticeable in the frequency range of 700 to 900 MHz. One concludes that horizontally polarized waves do not couple as well to the intermittent contact(s) that is (are) operative in the model tank.

A second series of experiments studied the aspect dependence of the modulation. In these experiments, the frequency was fixed at 850 MHz and the aspect angle was varied between 0 and 180 degrees, in 45-degree steps. Figure 13 shows the results for vertical polarization. Essentially, the modulation is largest for a narrow range of angles near 45 degrees. It is interesting to observe that, at this aspect angle, the contact between the sprocket and track is most "exposed" to the radar (Figure 10). More will be said about this below.

The aspect dependence obtained for horizontal polarization is shown in Figure 14. The modulation detected is smaller than that for vertical polarization, but it is observable over a larger range of angles. Perhaps this is because horizontally polarized waves couple only indirectly to the currents responsible for the observed modulation.

Since it appears that the sprocket-track contact must be exposed to the radar for modulation to be generated, an experiment was conducted to see if the modulation would diminish when the sprocket area was covered by a metal shield. Figure 15 shows this shield in place on the model. Data were again taken at 850 MHz with vertical polarization. The results obtained for the scattering amplitude as a function of time and aspect angle are shown in Figure 16. Comparison of Figure 16 with Figure 13 leads one to conclude that the shield essentially eliminates the intermittent-contact RADAM modulation. Because of the contracted

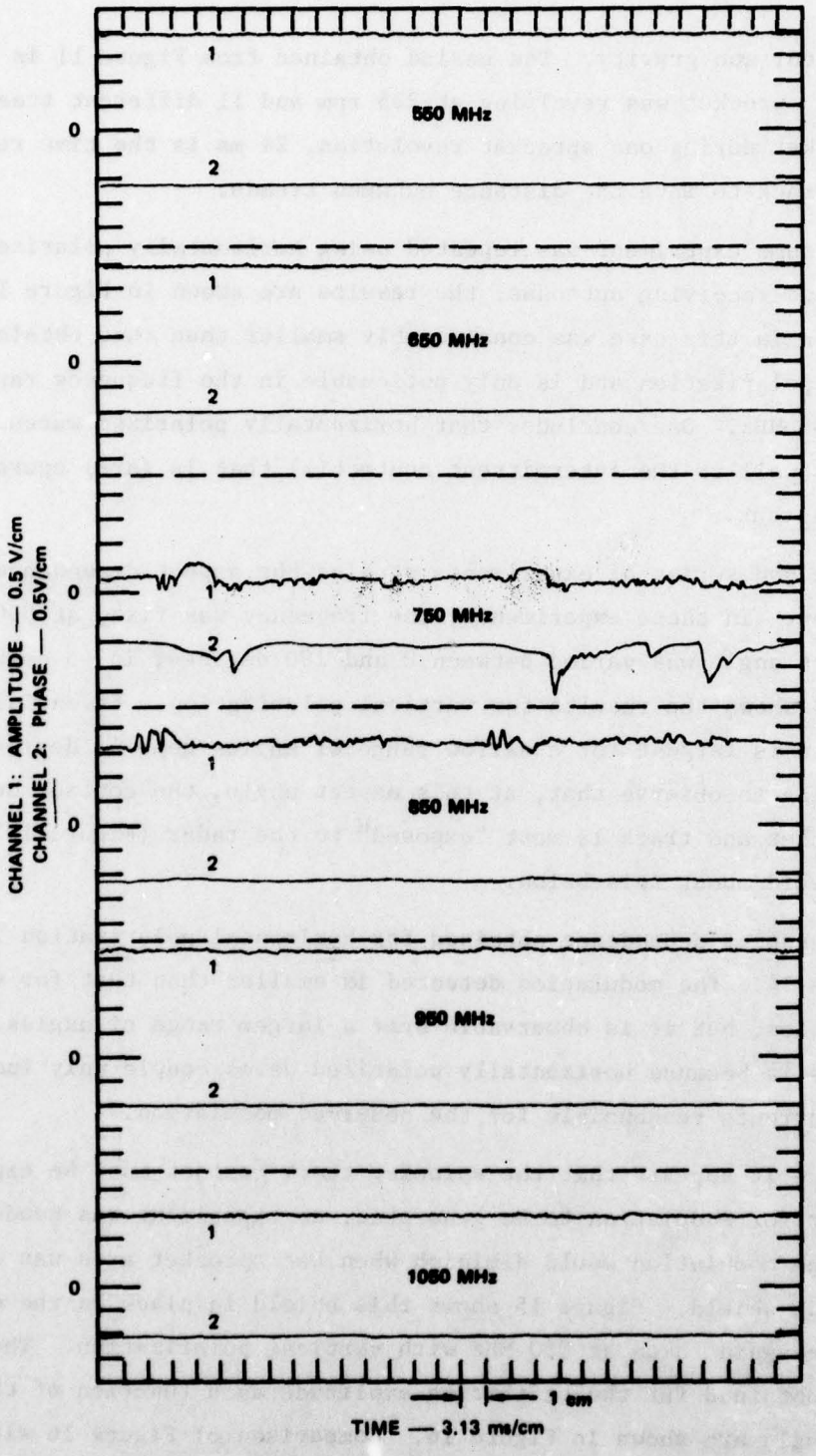

FIGURE 12 SCATTERING AMPLITUDE AND PHASE VERSUS TIME AND FREQUENCY FOR MODEL TANK (Horizontal Polarization, 45° Aspect)

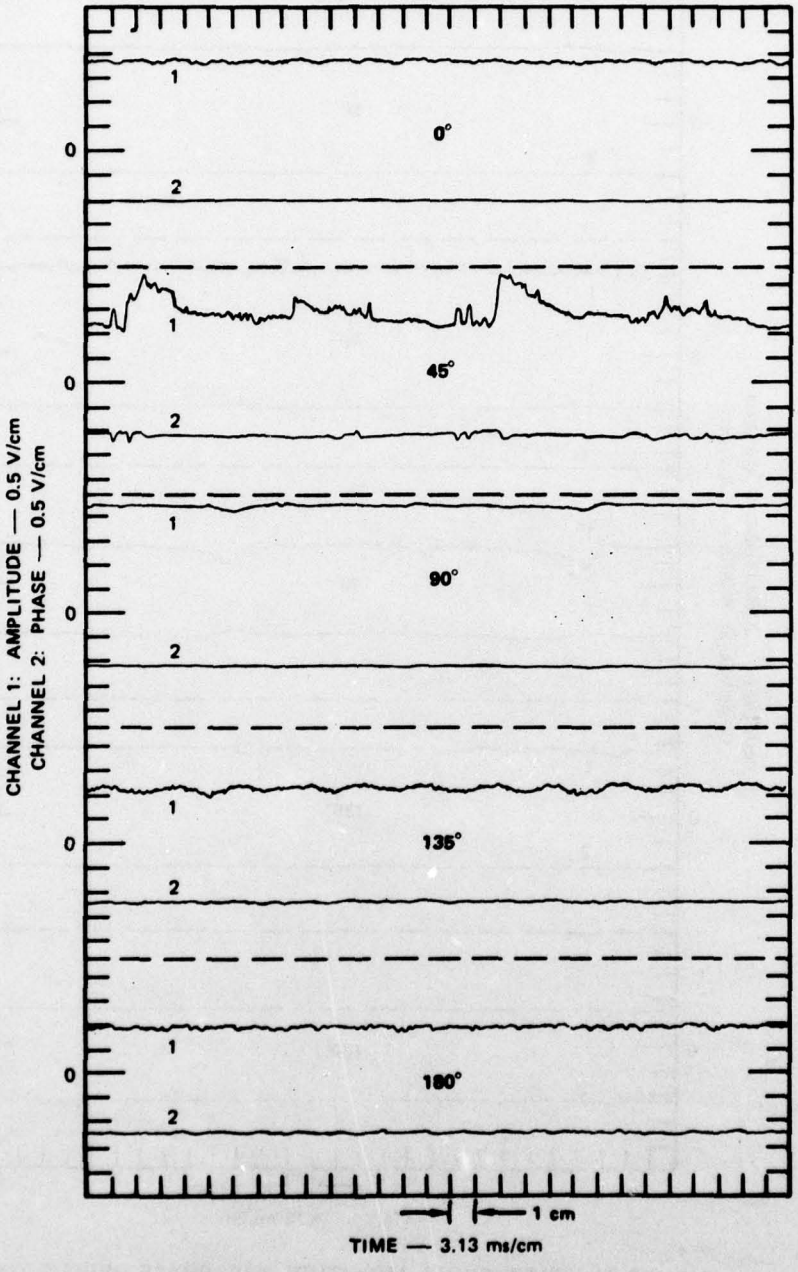

FIGURE 13 SCATTERING AMPLITUDE AND PHASE VERSUS TIME AND ASPECT ANGLE FOR MODEL TANK (Vertical Polarization, 850 MHz)

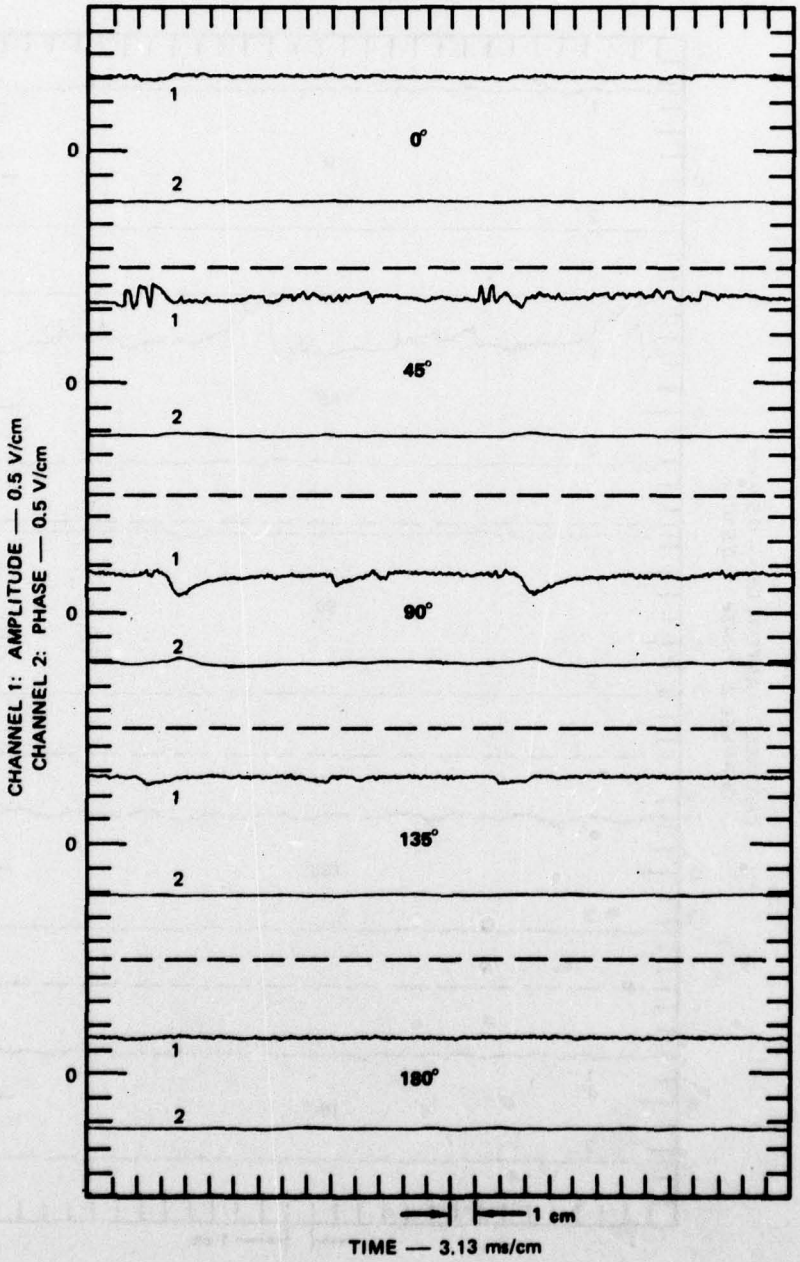

FIGURE 14 SCATTERING AMPLITUDE AND PHASE VERSUS TIME AND ASPECT ANGLE FOR MODEL TANK (Horizontal Polarization, 850 MHz)

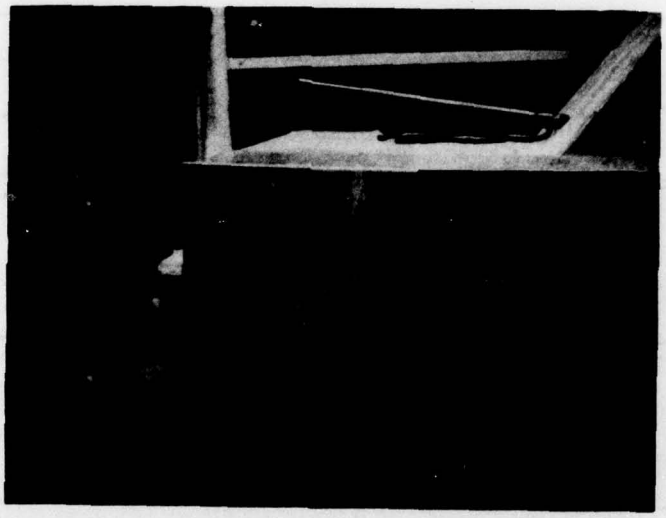

FIGURE 15 SPROCKET SHIELD

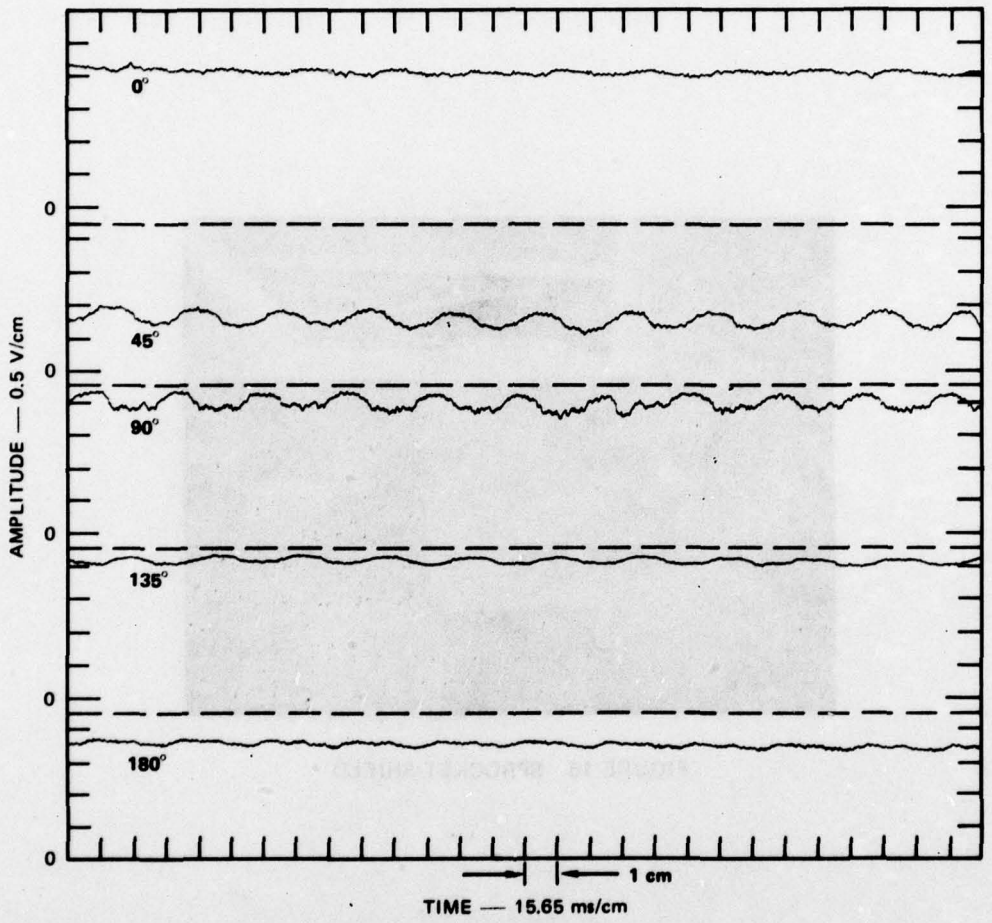

FIGURE 16 SCATTERING AMPLITUDE VERSUS TIME AND ASPECT ANGLE FOR MODEL TANK WITH SHIELDED SPROCKET (Vertical Polarization, 850 MHz)

time scale, a sinusoid-like modulation is apparent in Figure 16. This modulation is due to the change in the aspect of individual treads that occurs as the track moves along; it is smaller and more limited in spectral content than the intermittent-contact modulation observed without the shield.

The discussion so far has assumed that the source of the observed modulations is the contact(s) between the sprocket and the track. This assumption seems plausible because the sprocket is the sole connection between the track and the body of the model tank. However, to test this conjecture, the metal sprocket was replaced with a plastic (Delrin) one. Figure 17 shows the amplitude and phase of the scattering, as functions of time for metal and Delrin sprockets. In this experiment the frequency and aspect angle were 850 MHz and 45 degrees, and the range was nulled with the model tank in place to emphasize the modulation. It is very clear that the contact between the sprocket and the track is the source of RADAM in the model.

When one compares the RADAM waveforms produced by the metal sprocket on the model tank with the waveforms produced by a real tank (Figure 4), he notices that the pulse modulation produced by the model is not as "sharp-sided" as that produced by the real tank. This result is probably due to the way the sides of the sprocket on the model "rub" the drive chain during engagement; the sprockets on a real tank engage the tracks near the outer edges of the treads and contact is essentially made only on small areas of the faces of the sprocket teeth. Therefore, to more nearly model this type of contact, auxiliary contacting arms in contact with the track were added to the model. Besides providing a small contact area, the auxiliary contacting arms permitted the effect of contact location to be studied. Photographs of the contacting arms at three different locations on the track are shown in Figure 18. The contacting arms were spring loaded and connected to the tank body by braided metal straps attached to opposite ends of each arm.

Besides investigating the effect of contact location, one also wishes to know which parts of the track have the most effect on the frequency dependence of the observed RADAM modulation. There are only two basic

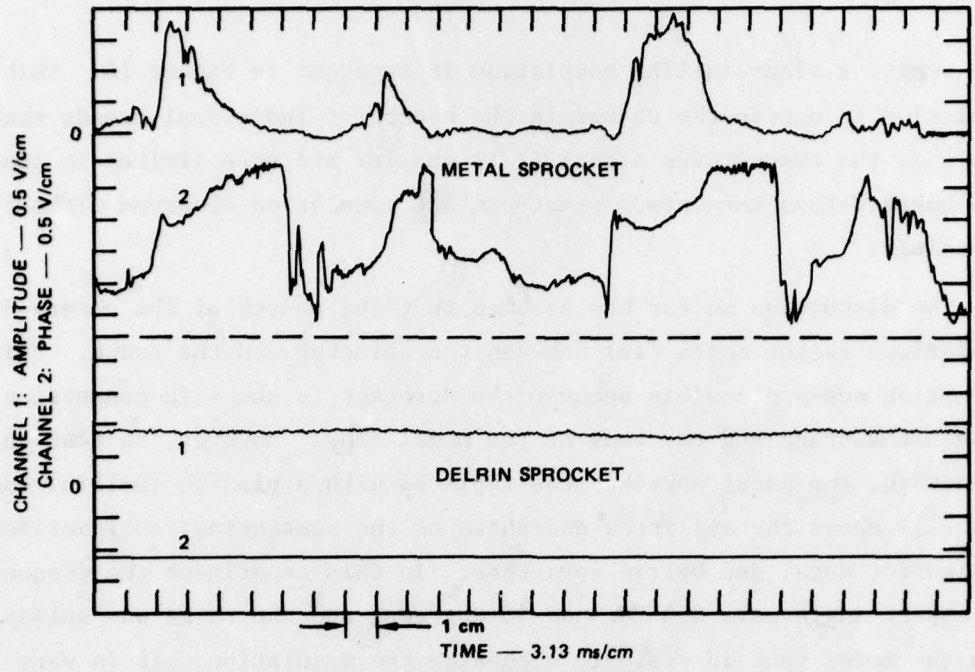

(a) VERTICAL POLARIZATION

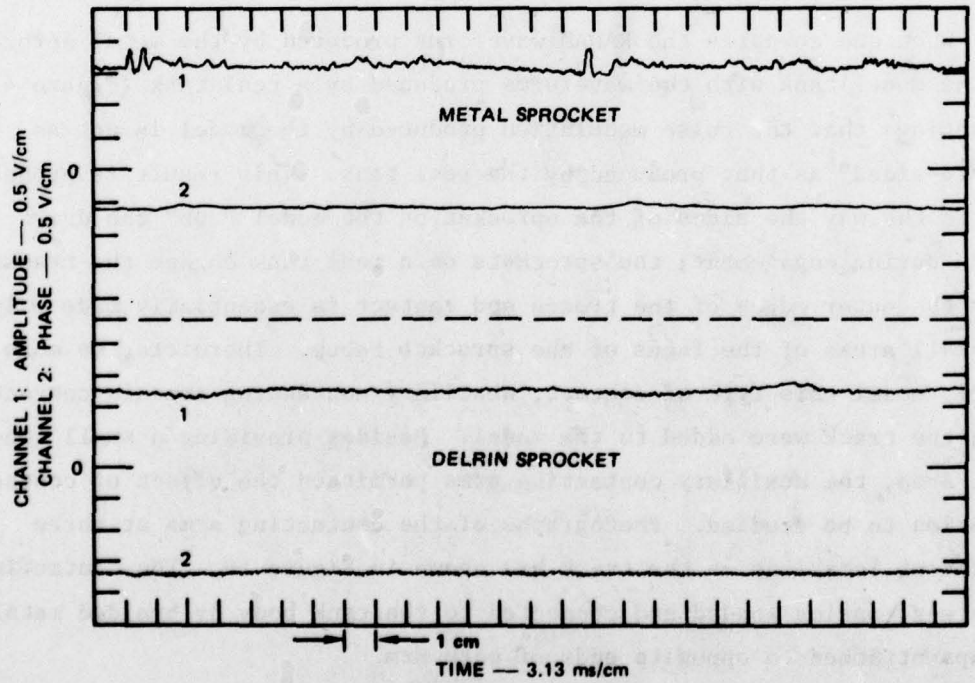

(b) HORIZONTAL POLARIZATION

FIGURE 17 SCATTERING AMPLITUDE AND PHASE VERSUS TIME FOR METAL AND DELRIN SPROCKETS (850 MHz, 45° Aspect)

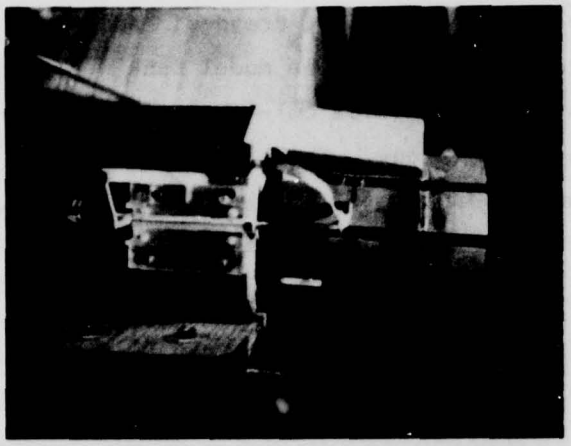

(a) CONTACTING ARM OUTSIDE OF TREADS

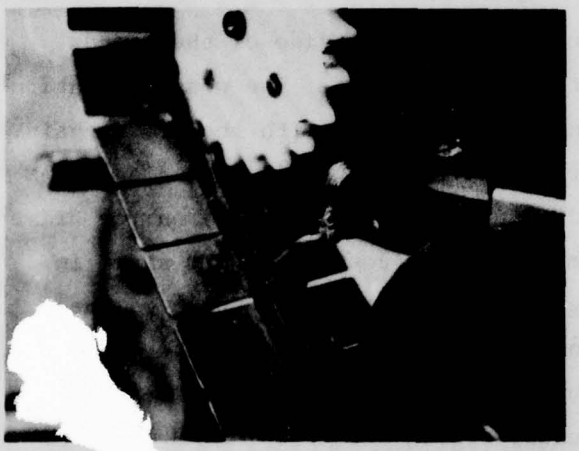

(b) CONTACTING ARM ON CONNECTING CHAIN NEAR SPROCKET (REAR OF MODEL TANK)

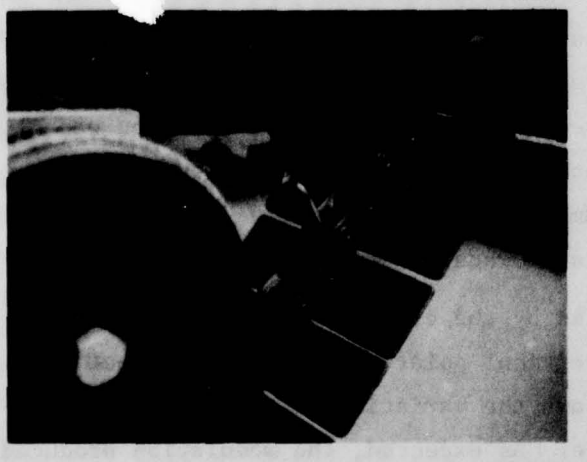

(c) CONTACTING ARM ON CONNECTING CHAIN NEAR FRONT OF MODEL TANK

FIGURE 18 POSITIONS OF AUXILIARY CONTACTING ARMS

parts to the track: the individual treads and the drive chain that connects the treads together. To study the effect of tread dimensions, the plates ("treads") on the conveyor belt used in the model tank were modified to three different lengths: 2.75 in (6.99 cm)--short, 4.50 in (11.43 cm)--medium, and 6.50 in (16.51 cm)--long. These plates were arranged on the belt to pass the contact in the following order: 13 long, 15 medium, 10 short, and 32 medium, for a total of 70 treads.

Several experiments involving these different contacting arms and modified track were carried out. Frequency, aspect angle, and polarization were varied in the experiments, and the Delrin sprocket was used in all cases.

When the contacting arm was located on the outside of the treads [Figure 18(a)], very little modulation was observed. The weak modulation observed was strongest when the contact was in line with the drive chain. This result suggests that the major currents involved in producing RADAM in the model tank flow on the inside of the treads, probably on the drive chain. This suggestion was confirmed when the contacting arm shown in Figure 18(b) was used. A large degree of modulation was observed when contact was made with the drive chain near the sprocket. Hence, it appears that the currents carried by the track as a whole, rather than those carried on the individual treads, are important to RADAM.

Experiments were also conducted with the contacting arm located at the opposite end of the track, as shown in Figure 18(c). Even though contact is also made with the drive chain, the observed modulation was relatively weak. Hence, the currents on the track on the front and back of the tank are apparently not symmetric. This asymmetry is probably at least partially caused by the bistatic radar.

The largest modulation produced by the contacting arrangement of Figure 18(b) again occurred with vertical polarization and an aspect angle of 45 degrees. Figure 19 shows the variation of scattering as a function of frequency for this case. As expected, the modulation produced by the auxiliary contact appears more "pulse-like" than that produced by the metal sprocket. In addition, the largest modulation is confined to

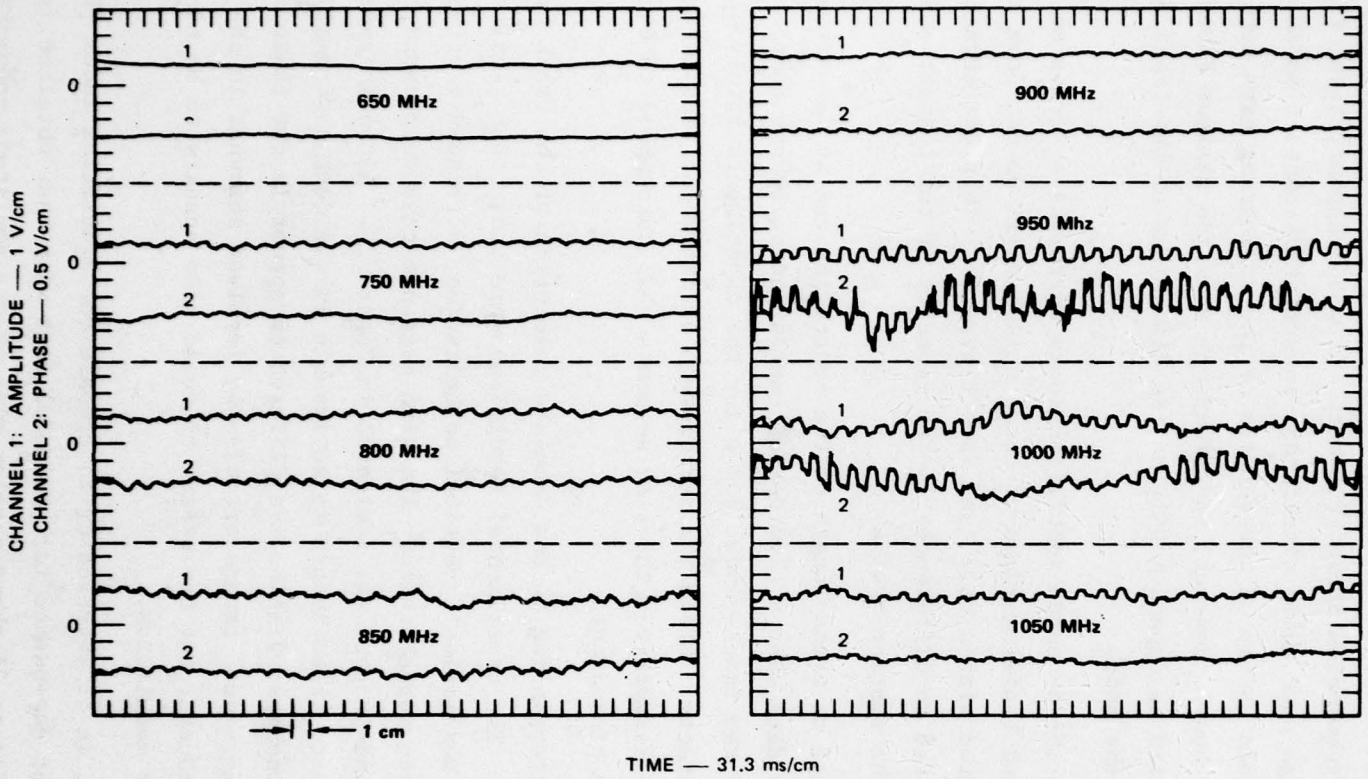

FIGURE 19 SCATTERING AMPLITUDE AND PHASE VERSUS TIME AND FREQUENCY FOR MODEL TANK WITH AUXILIARY CONTACT (Vertical Polarization, 45° Aspect)

a narrower frequency range than when the metal sprocket was used. It can be seen in Figure 19 that the degree of modulation definitely begins to decrease at frequencies above 1000 MHz. It would appear, then, that the frequency range over which significant intermittent-contact RADAM is observed depends partly on the details of the connecting path between the track and the body. However, the frequency at which maximum RADAM is observed appears to depend mostly on the dimensions of the track as a whole and of the body.

Although the detected modulation looks more like a series of pulses, the leading and trailing edges of these pulses still do not look like those associated with a real tank (see Figure 6). This difference is probably related to differences in the geometry of the contact and the dynamics of the contact motion.

The effect of tread length on the scattering can be determined by examining the data over a time period corresponding to one complete revolution of the track--about 2.5 s for the experiments involving the auxiliary contacts. Since the arrangement of different tread lengths on the track was asymmetric, the time segments that correspond to each tread length can be picked out.

Data corresponding to one complete revolution of the track are shown in Figure 20. The experimental conditions were those that resulted in the greatest modulation: vertical polarization, a frequency of 950 MHz, and a 45 degree aspect angle. The time segments that correspond to different tread lengths are indicated in Figure 20. Although some variation due to tread length is noticeable in the degree of amplitude modulation, the most distinctive differences appear in the phase modulaton. Hence, the individual treads are clearly involved somewhat in the scattering process, but the effect of tread size appears to be minor for the amplitude modulation.

Finally, it is interesting to compare the modulation index [Eq. (4)] and its aspect dependence for the model tank with that obtained for the real tank. Figure 21 shows a polar plot of the amplitude modulation index for the model tank as a function of aspect angle. The corresponding

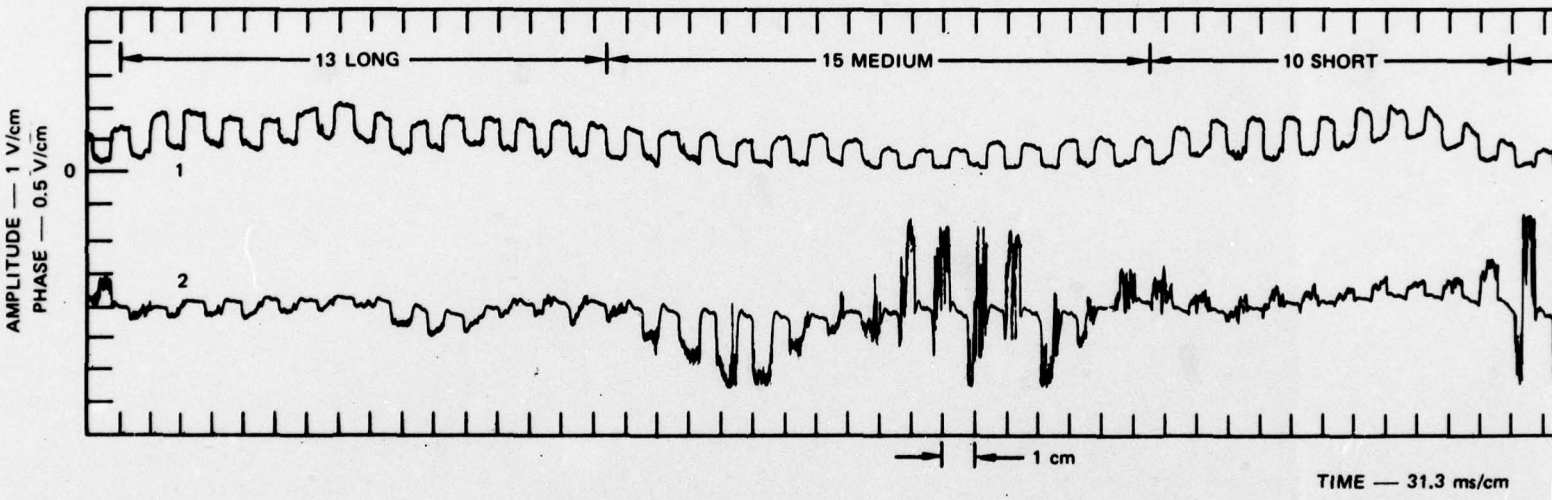
13 LONG
15 MEDIUM
10 SHORT
AMPLITUDE — 1 V/cm
PHASE — 0.5 V/cm
0
1
2
1 cm
TIME — 31.3 ms/cm

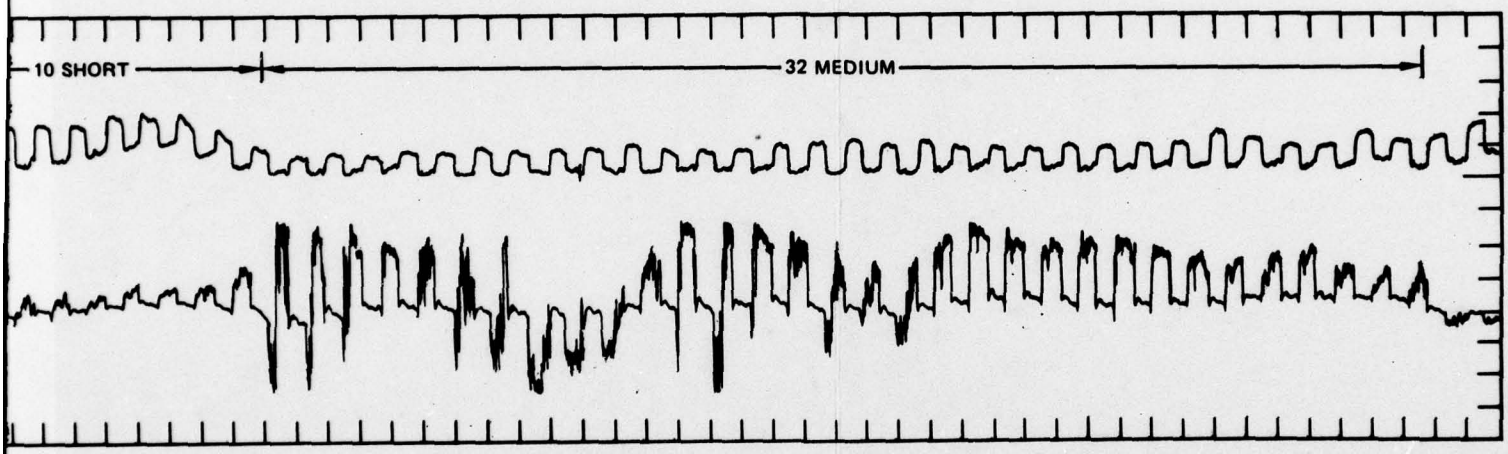

TIME — 31.3 ms/cm

FIGURE 20 SCATTERING AMPLITUDE AND PHASE VERSUS TIME FOR THE MODEL TANK WITH DIFFERENT LENGTH TREADS (Vertical Polarization, 950 MHz, 45° Aspect)

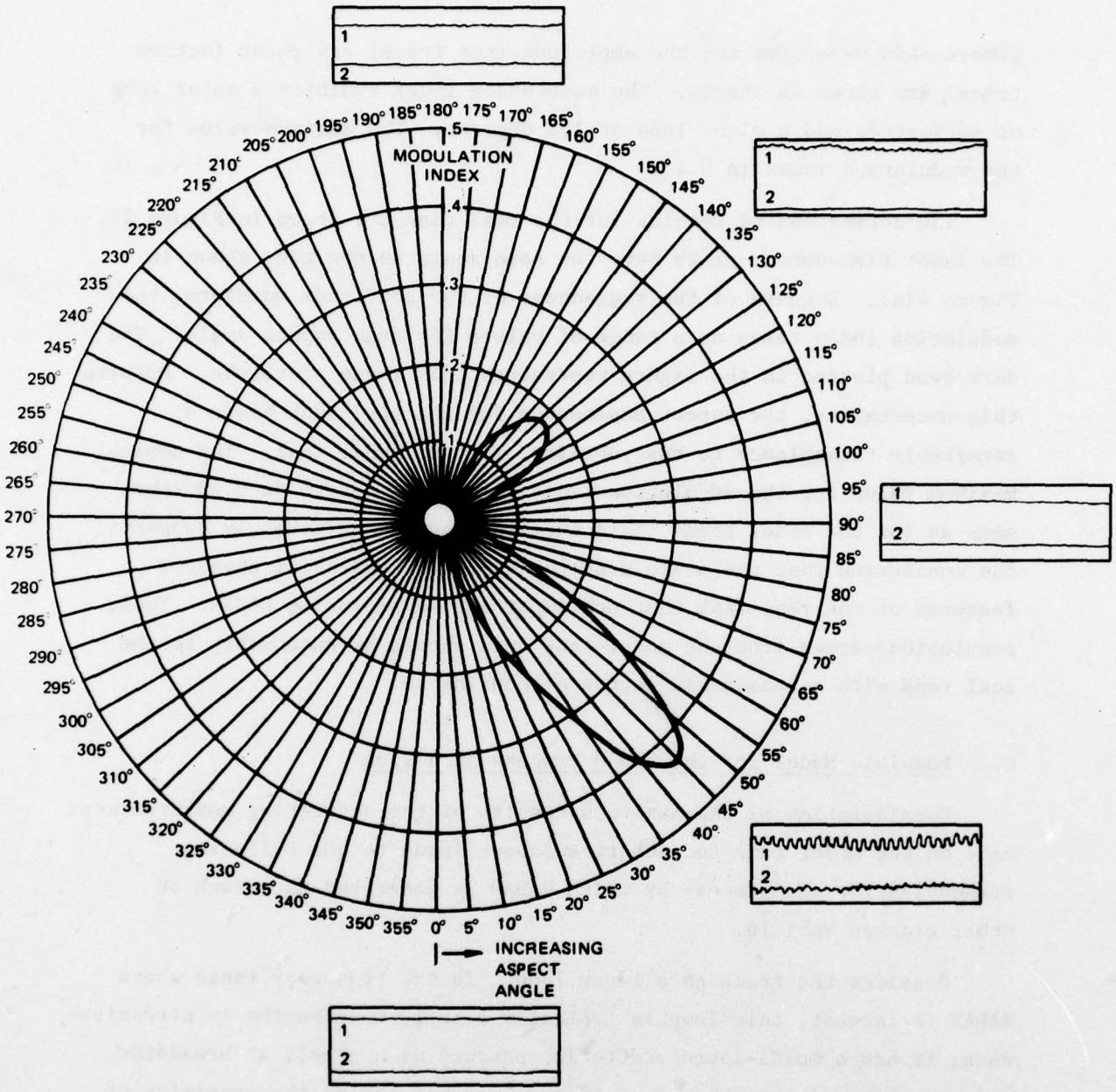

FIGURE 21 RADAM MODULATION VERSUS ASPECT ANGLE FOR MODEL TANK
(Vertical Polarization, 950 MHz)

time-domain waveforms for the amplitude (top trace) and phase (bottom trace) are shown as insets. The modulation index exhibits a major lobe at 45 degrees and a minor lobe at 135 degrees. The maximum value for the modulation index is 0.43.

The corresponding results for the real tank are shown in Figure 22. The inset time-domain plots have the same scale as the plot shown in Figure 4(a). Because of the raggedness of the amplitude waveform, the modulation index takes on a range of values for each aspect angle. The dark band plotted in the figure represents this range of values. Despite this uncertainty, the aspect dependence for the real tank bears a remarkable resemblance to that obtained for the model tank. The nominal maximum value for the modulation index even turns out to be 0.43--the same as for the model tank! This excellent agreement strongly supports the conclusion that the scale model contains the essential physical features of the real tank that are important in producing RADAM. Thus, conclusions drawn from the model tank data should be extendable to the real tank with a reasonable degree of confidence.

C. Possible Model for the RADAM Process in a Tank

Consideration of the numerous results of the scattering measurements made on the model tank and described above leads to the following suggestion for the process by which RADAM is generated in a tank or other tracked vehicle.

Consider the track as a large loop. In the frequency range where RADAM is largest, this loop is typically 5 to 10 wavelengths in circumference; it has a multi-lobed scattering pattern with a null at broadside, reduced scattering in the plane of the loop because of the proximity of the tank body, and, of course, nulls between each lobe. If the induced currents flowing on this loop are strongly perturbed, the lobe pattern will shift. Hence, a possible explanation for the very large degree of modulation observed is that the perturbation produced by the intermittent contact between the body and the track via the sprocket causes the lobe pattern to switch between a peak and a null in the direction of observation. Because of the fixed minima in the pattern for broadside and end-on

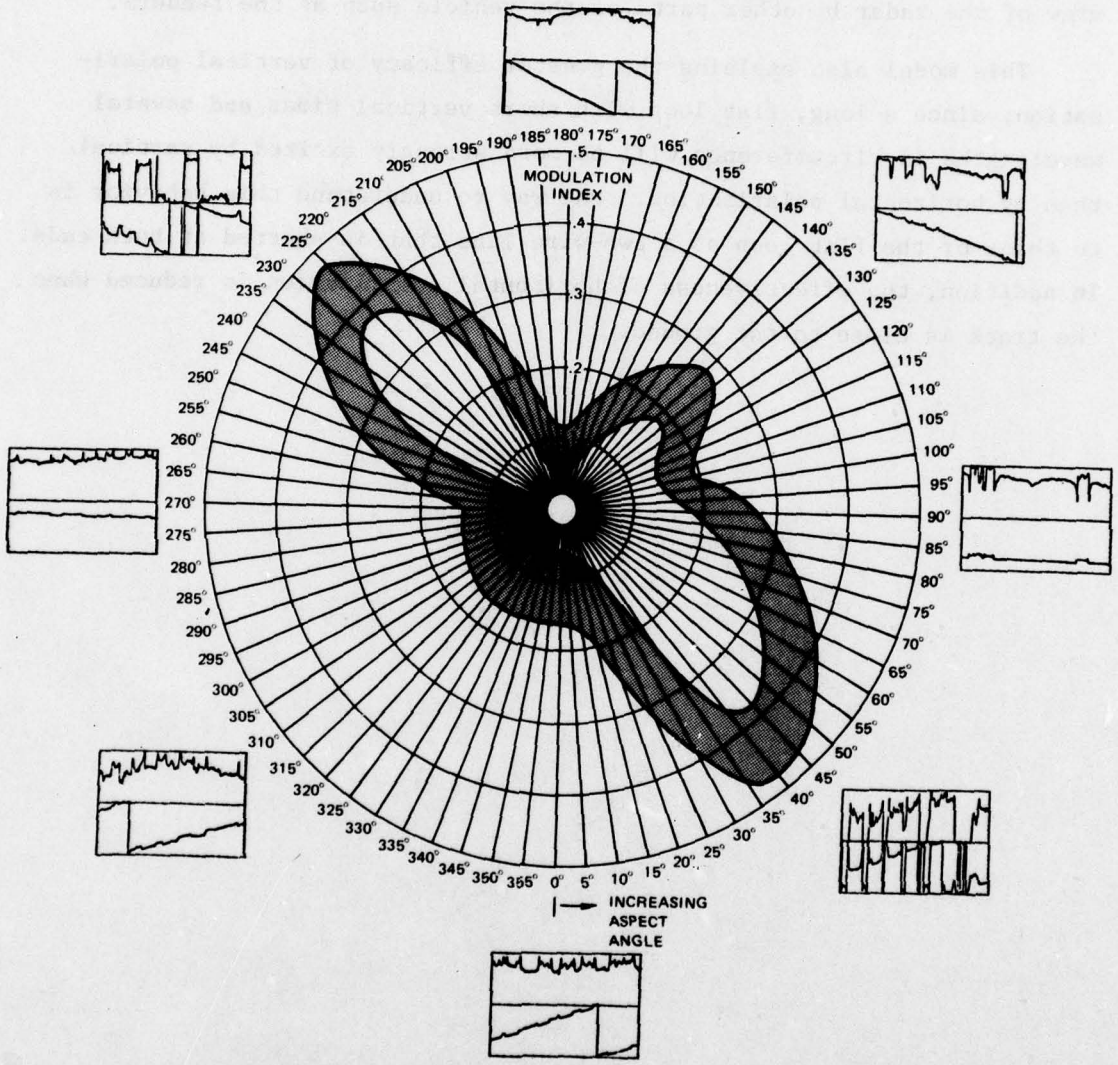

FIGURE 22 RADAM MODULATION VERSUS ASPECT ANGLE FOR FULL-SCALE TANK (Vertical Polarization, VHF)

observations, the lobe-switching effect should be most noticeable for observation angles of 45, 135, 225, and 315 degrees. This is observed, but the effect is not equally strong in these four directions. This asymmetry is probably caused by the sprocket being blocked from field of view of the radar by other parts of the vehicle such as the fenders.

This model also explains the greater efficacy of vertical polarization, since a long, flat loop with short vertical sides and several wavelengths in circumference will be more strongly excited by vertical than by horizontal polarization. One way to understand this behavior is to think of the flat loop as a two-wire line that is shorted at both ends. In addition, the effectiveness of horizontal polarization is reduced when the track is close to the ground.

V. IDENTIFICATION OF TRACKED VEHICLES BY TIME-DOMAIN PROCESSING OF RADAM WAVEFORMS

As discussed in Section III, the RADAM modulation produced by tracked vehicles appears quite distinctive in the time domain, and thus, this modulation should be useful for identifying these vehicles. To do so, one needs to develop a RADAM signature from this modulation. One way to do this might be to identify the times at which the two types of transients (the opening and closing of a contact) occur and then to measure the differences between these times. These time differences, suitably normalized with respect to vehicle speed, should serve as a RADAM signature. Some preliminary results that show the feasibility of generating distinct signatures are presented in this section for different types of vehicles.

For the purposes of the preliminary demonstration, a time-domain processor that used a simple algorithm for detecting the opening and closing of a contact was built and tested. In this algorithm, if the initial part of the bipolar impulse at the output of the bandpass filter was positive [Figure 8(a)], the event was defined as a contact opening. Then, given such a positive impulse, a negative impulse was defined as a contact closing. To avoid confusion in this scheme, the smaller negative pulse that immediately follows a positive "opening" pulse was blanked. For some data, this definition of opening and closing impulses appears to agree with the physical situation, and for others it does not. However, this algorithm was used for the first experiments because it simplified the processor hardware.

Figure 23 shows a block diagram of this simplified version of a time-domain RADAM processor. The system was designed to process data recorded in the form of a modulated 10-kHz carrier on analog tape. A time-code track on the tape was used for locating particular data segments, and the time-code signal was also used to initiate processing.

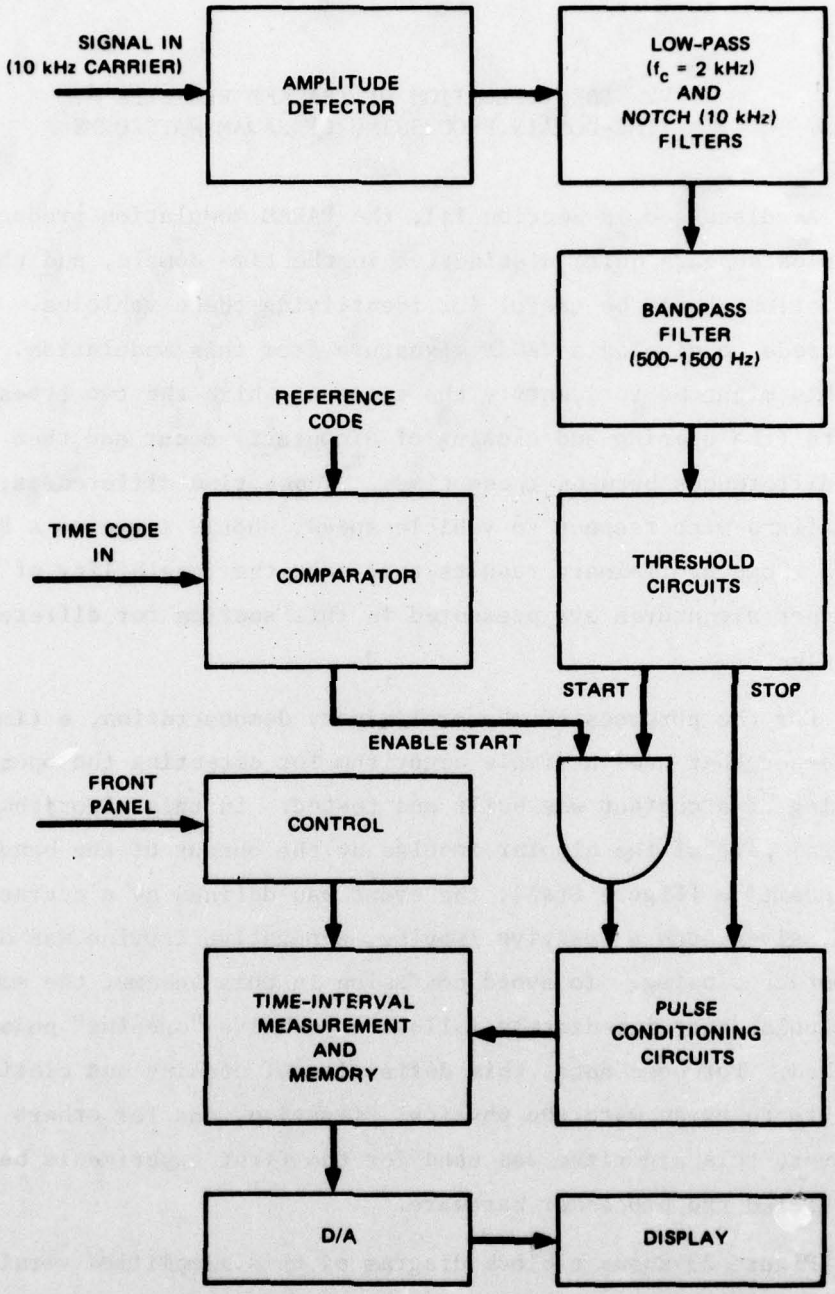

FIGURE 23 BLOCK DIAGRAM OF SIMPLIFIED TIME-DOMAIN RADAM PROCESSOR

Threshold circuitry was used to discriminate against clutter signals that were smaller than the bona fide start and stop impulses produced by the opening and closing of a contact. After these start and stop impulses passed through the threshold circuits, they triggered pulse-conditioning circuits that generated trains of square pulses in which the length of each square pulse was equal to the time between the corresponding pair of start and stop impulses. Each pulse length was then measured, and the results were stored in 1 of 32 bins that covered a range of 1 through 32 ms in 1-ms steps. Pulse lengths over 32 ms were stored in the 32-ms bin. When the lengths of 128 square pulses had been measured (or when the processing was terminated by the operator) the results in memory were displayed on an oscilloscope as a histogram of the time durations between the start and stop impulses identified by the algorithm. This histogram can be called a RADAM signature.

The results of using this system to process some selected scattering data for a tank and an APC are shown in Figure 24. Figure 24(a) shows the pulse-length distribution for a tank. There is a clear preponderance of pulses near 17 ms, as well as some pulses with lengths greater than 32 ms. The pulse-length distribution for an APC [Figure 24(b)] shows a preponderance of pulses in the 4 to 6 ms range. For these data, then, an operator viewing the display can clearly distinguish the two types of vehicles.

The previous results used data taken at two different aspect angles. Data taken at the same aspect angle were also compared. The results for a tank, APC, and truck are shown in Figure 25. All were obtained using VHF, vertical polarization, and a 225-degree aspect angle. The results for the tank and APC are similar to those shown in Figure 24. The truck exhibits only a few RADAM events, and the corresponding pulse lengths are fairly evenly distributed. Again, all three RADAM signatures are clearly distinguishable.

Although questions regarding the statistical prevalence and uniqueness of these RADAM signatures among vehicles of a given class remain, the preliminary results given here strongly suggest that the time-domain processing of RADAM signals for real-time target identification deserves further study.

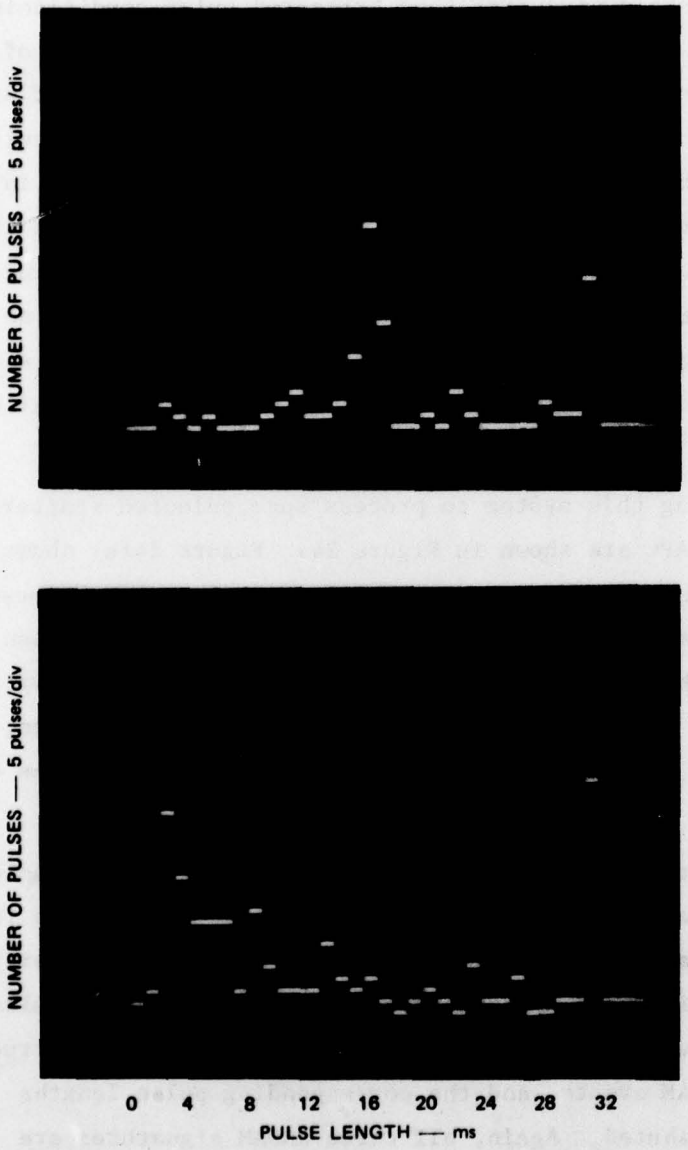

FIGURE 24 RADAM SIGNATURES FOR A TANK AND AN APC

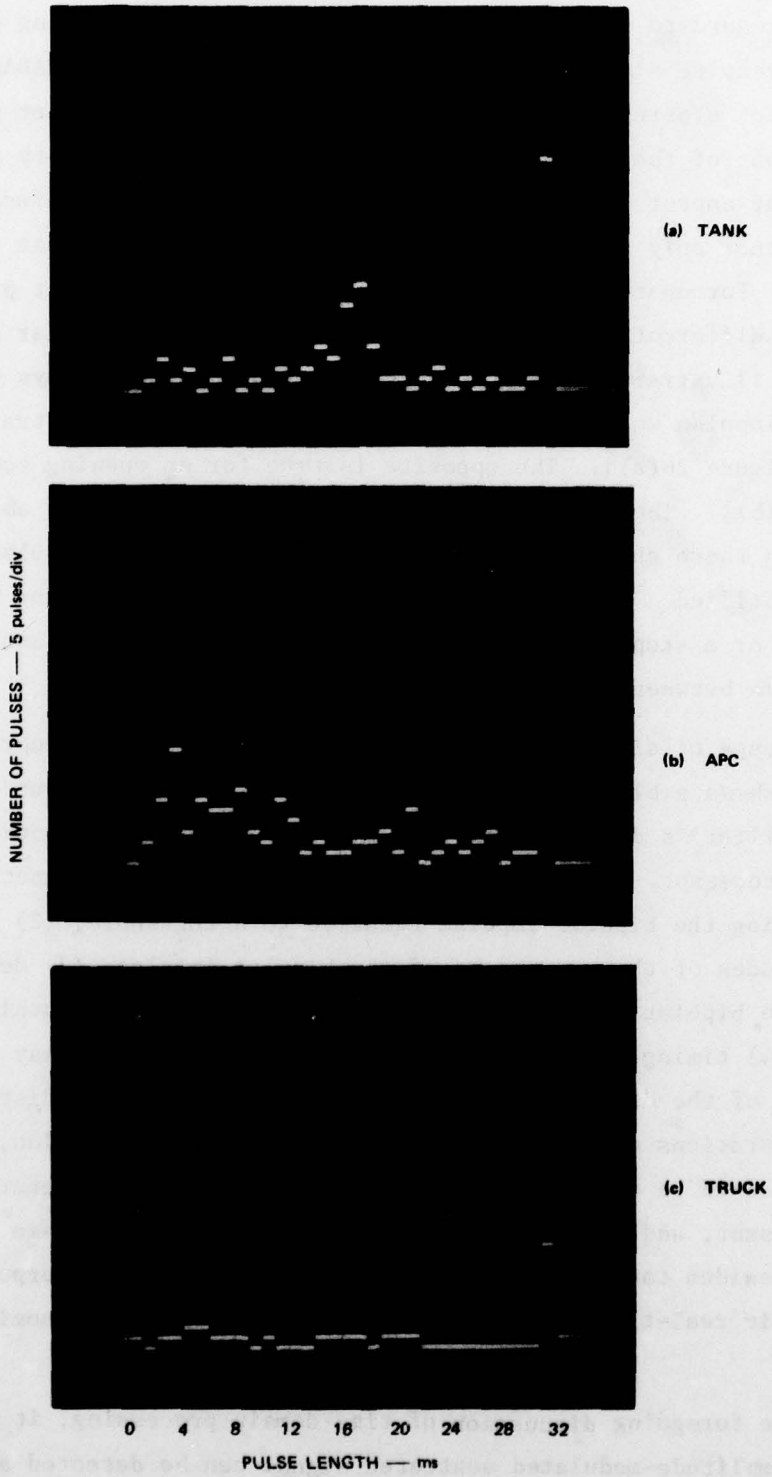

FIGURE 25 RADAM SIGNATURES FOR A TANK, AN APC, AND A TRUCK

With regard to the processor itself, real-time processing of real data will require a more general algorithm because a given RADAM event, say a contact closing, can produce a bipolar impulse of either polarity at the output of the bandpass filter. This polarity ambiguity comes from the changing aspect of the target. This situation would confuse the simple algorithm that only compares the polarity of the impulses that exceed the threshold. Fortunately, the closing and opening of a contact produce distinctly different bipolar impulses. These distinct bipolar characteristics are illustrated in Figure 26. A closing contact always produces a bipolar impulse whose leading impulse is smaller than the trailing impulse [Figure 26(a)]. The opposite is true for an opening contact [Figure 26(b)]. Therefore, the required algorithm should be able to distinguish these characteristics so that start and stop impulses are always identified. It is immaterial whether a contact closing is defined as a start or a stop, since both the time between the start and a stop and the time between a stop and a start would be measured.

This type of algorithm is best implemented using a microprocessor. Figure 27 shows a block diagram for such a system. The output of the bandpass filter is digitized and fed into a buffer memory controlled by the microprocessor. The microprocessor would perform the functions of (1) detecting the bipolar impulse relative to a threshold, (2) comparing the magnitudes of the components of the bipolar impulse, (3) deciding whether the bipolar impulse corresponds to the closing or opening of a contact, (4) timing, (5) sorting, (6) storage, and (7) display control. The output of the display might be a histogram showing the distribution of pulse durations or intervals. For more automatic operation, this RADAM signature could be correlated with a library of stored signatures by the microprocessor, and the final display could be simply the name of the target. Besides target identification for reconnaissance purposes, such an automatic real-time processor should also be useful for homing applications.

In the foregoing discussion of time-domain processing, it was assumed that the amplitude-modulated scattered signal can be detected and distinguished from the noise and clutter and that the rapid transients

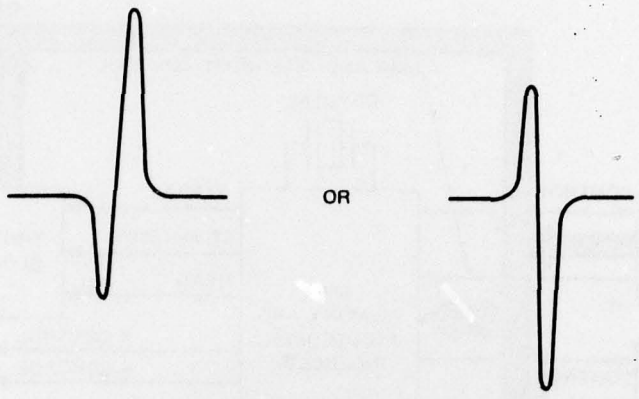

(a) START: CONTACT CLOSING

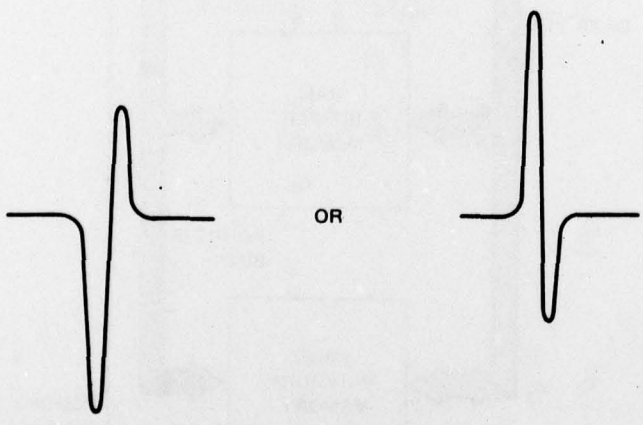

(b) STOP: CONTACT OPENING

FIGURE 26 "START" AND "STOP" BIPOLAR IMPULSES

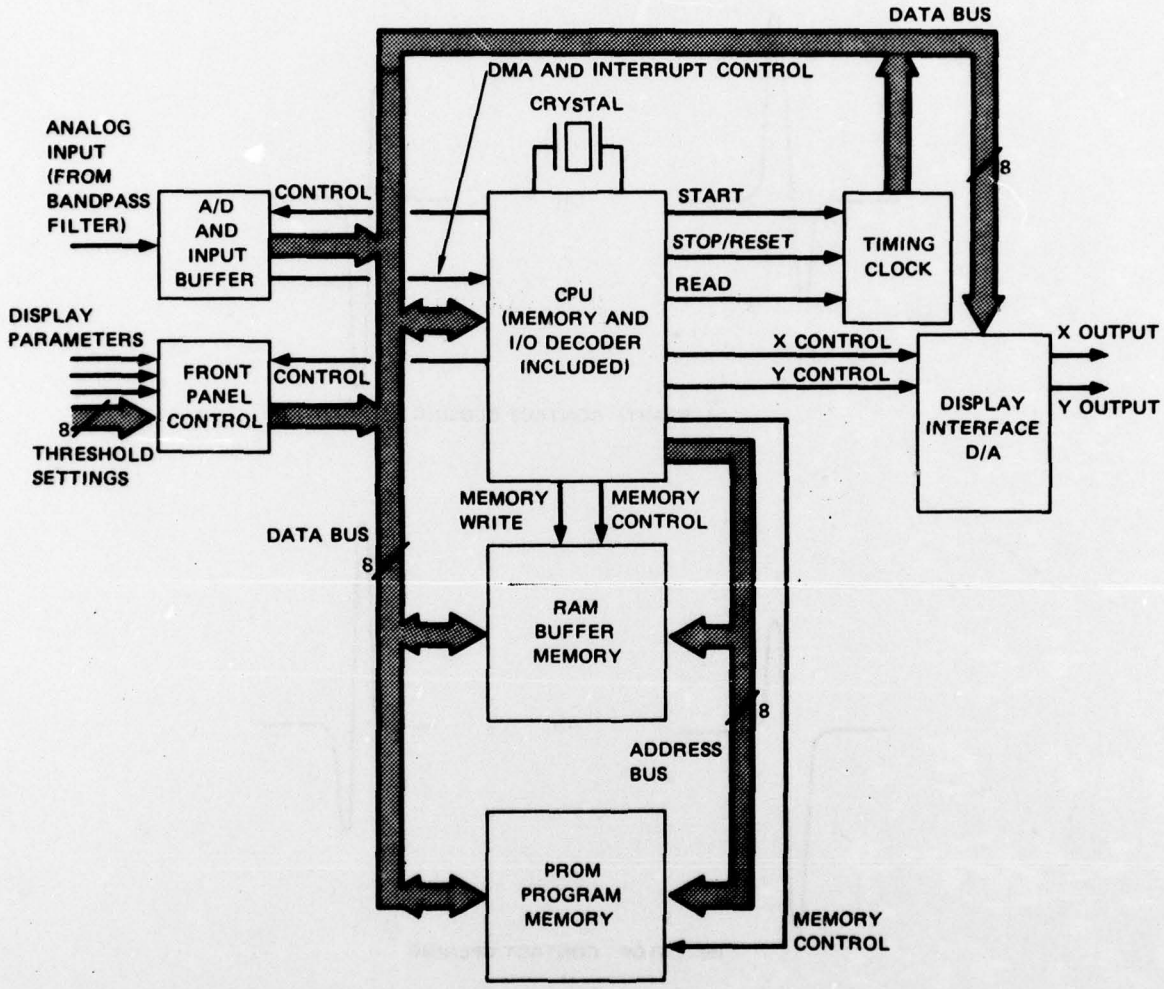

FIGURE 27 BLOCK DIAGRAM OF REAL-TIME RADAM PROCESSOR

produced by RADAM are faithfully reproduced in the receiver. These conditions were always true in both the laboratory and field experiments where a CW radar and bandwidths between 2 and 20 kHz were used. In practice, however, the radar is likely to be operated in a pulsed mode. Therefore, it is worthwhile to consider how this operating mode would affect RADAM processing.

Basically, the amplitude modulated radar waveform samples the "waveform" of the time-varying radar cross section (RCS) of the target. To faithfully recontruct the rapid variations in RCS associated with RADAM, the sampling rate (pulse-repetition rate) must be equal to at least twice the reciprocal of the duration of the transient. This transient duration is typically 1 ms for the RADAM waveforms produced by the tracked vehicles examined so far; so the sampling rate should be at least 2 kHz, but 4 kHz would be better. However, more data are needed for tracked vehicles before a minimum allowable pulse-repetition frequency for tracked vehicles can be established.

Each radar pulse must be detectable above noise and clutter. Achievement of this condition depends on the effective peak transmitter power, duty factor, antenna gain, range, target RCS, receiver sensitivity, and clutter environment. Chirped signals or phase-coded bursts can be used if they repeat at the minimum allowable sampling frequency.

VI. CONCLUSIONS AND RECOMMENDATIONS

Under this contract during the past three years, the original goals of the research program have been successfully achieved:

1. To identify and isolate the physical processes and mechanisms that contribute to an intermittent-contact RADAM signature,
2. To identify and explain important recognizable features of the signature, and
3. To determine means for separating the significant identifying components of the signature from nonmeaningful components.

Specifically, the following conclusions were derived from this work:

- The rapid variations in the scattering from a moving multielement target are produced by variations in surface currents caused by intermittent contacts between the target elements.
- A moving multielement target with intermittent contacts can be modeled as a loaded scatterer with time varying load impedances.
- The radio-frequency dependence of the modulation produced by intermittent-contact RADAM is determined by (1) the ratio of the target dimensions to the electromagnetic wavelength, and (2) the frequency dependence of the impedances associated with the contacts on the target.
- The degree of modulation depends on the locations of the contacts within the target, on the dynamics of contact motion, and on whether or not the contacts act in concert.
- Modulation produced by the motion of target elements can be identified by its sinusoid-like nature; modulation produced by intermittent contacts is more rapid and similar to a square wave.
- These distinctive features permit rejection of the modulation due to element motion by simple bandpass filtering.
- The rapid modulation transients associated with intermittent-contact RADAM are produced only when the contacts are conductive. The modulation is less rapid and is reduced in magnitude if the contacts are capacitive or lossy. However, the presence of mud or grease in the contact area does not appear to be a problem because the contacting elements easily break through these materials.
- Tracked vehicles exhibit much RADAM modulation in the VHF range. The modulation has the characteristics expected for a single

contact and occurs aperiodically. The question of whether such intermittent contact modulation can be detected at higher frequencies remains to be answered.

- Studies of the UHF scattering from a 5:1 scale-model tank suggest that the source of RADAM modulation in a tracked vehicle is the intermittent contact between the sprocket attached to the tank body and the track.
- A major component of current involved in the RADAM process in a tracked vehicle is the current flowing on the track as a whole. The modulation depends only weakly on the size of an individual tread.
- A possible explanation for way in which the RADAM modulation produced by a tracked vehicle varies as a function of frequency, aspect angle, and polarization can be obtained by considering the track to be a large, flat loop that is connected and disconnected to the body of the tank.
- It appears that some of the aspect dependence of RADAM is caused by various parts of the vehicle shadowing the contacts from the radar.
- The opening and closing of a contact on the target can be unambiguously distinguished by the characteristics of the bipolar pulse produced at the output of a bandpass filter by each corresponding transient.
- Using bandpass filtering and measurement of the time between the opening and closing of a contact, or vice versa, one can develop distinct RADAM signatures for different kinds of tracked vehicles. Use of this signature should permit real-time identification of this type of vehicle.
- The electronics required for a real-time tracked-vehicle identification system are relatively simple, inexpensive, small, and lightweight and should be easily retrofitted to an existing radar. Additional radar requirements, besides that it be operable at a suitable radio frequency, are that it have a sufficiently high pulse-repetition frequency (the minimum required pulse-repetition frequency not yet determined) and adequate single-pulse sensitivity.

These results and conclusions are based on very limited data. Before practical exploitation of RADAM is attempted, it is recommended that a statistically significant data base for full-scale tracked vehicles in a field environment be collected and analyzed. Further studies of the source of the RADAM modulation, and of the effect of vehicle speed and contact contamination on the RADAM signature, should also be conducted for full-scale vehicles.

REFERENCES

1. A. J. Bahr and J. P. Petro, "Experimental Comparison Between Induced Surface Current and Scattered Electromagnetic Waves for a Metal Target with Time-Varying Characteristics," Electronics Letters, Vol. 13, pp. 777-778 (December 1977).

2. R. F. Harrington, "Theory of Loaded Scatterers," Proc. IEE, Vol. 111, p. 617-623 (April 1964).

3. J. K. Schindler, R. B. Mack, and P. Blacksmith, Jr., "The Control of Electromagnetic Scattering by Impedance Loading," Proc. IEEE, Vol. 53, 993-1004 (Aug. 1965).

4. A. J. Bahr and J. P. Petro, "On the RF Frequency Dependence of the Scattered Spectral Energy Produced by Intermittent Contacts Among Elements of a Target," IEEE Trans. Antennas Propagat., Vol. AP-26, pp. 618-621 (July 1978).

5. A. J. Bahr, V. R. Frank, J. P. Petro, and L. E. Sweeney, Jr., "Radar Scattering from Intermittently Contacting Metal Targets," IEEE Trans. Antennas Propagat., Vol. AP-25, pp. 512-518 (July 1977).

6. V. R. Frank, J. P. Petro, and A. J. Bahr, "Backscattering from a Cylindrical Dipole Centrally Loaded by a Time-Varying Impedance," IEEE Trans. Antennas Propagat., Vol. AP-25, pp. 356-358 (May 1977).

7. Y. Y. Hu, "Backscattering Cross Section of a Center-Loaded Cylindrical Antenna," IRE Trans. Antennas Propagat., Vol. AP-6, pp. 140-148 (January 1958).

8. 

UNCLASSIFIED

SECURITY CLASSIFICATION OF THIS PAGE (When Data Entered)

REPORT DOCUMENTATION PAGE	READ INSTRUCTIONS BEFORE COMPLETING FORM
1. REPORT NUMBER: AFOSR-TR- 78-1507	2. GOVT ACCESSION NO. / 3. RECIPIENT'S CATALOG NUMBER
4. TITLE (and Subtitle): ANALYSIS OF RADAR DETECTION OF AGITATED METALS (RADAM)	5. TYPE OF REPORT & PERIOD COVERED: Final Report Covering the Period 1 April 1977 to 15 July 1978
	6. PERFORMING ORG. REPORT NUMBER: SRI Project 4176
7. AUTHOR(s): A. J. Bahr, V. R. Frank, J. P. Petro, L. E. Sweeney, Jr., O. G. Villard, Jr.	8. CONTRACT OR GRANT NUMBER(s): F44620-75-C-0046
9. PERFORMING ORGANIZATION NAME AND ADDRESS: SRI International, Menlo Park, California 94025	10. PROGRAM ELEMENT, PROJECT, TASK AREA & WORK UNIT NUMBERS: 61102F, 2305B2
11. CONTROLLING OFFICE NAME AND ADDRESS: Air Force Office of Scientific Research (AFOSR/NE), Bldg. 410, Bolling AFB, Washington, D.C. 20332	12. REPORT DATE: September 1978 / 13. NO. OF PAGES: 64
14. MONITORING AGENCY NAME & ADDRESS (if diff. from Controlling Office)	15. SECURITY CLASS. (of this report): UNCLASSIFIED
	15a. DECLASSIFICATION/DOWNGRADING SCHEDULE: N/A

16. DISTRIBUTION STATEMENT (of this report)

Approved for Public Release; Distribution Unlimited.

A041713

17. DISTRIBUTION STATEMENT (of the abstract entered in Block 20, if different from report)

18. SUPPLEMENTARY NOTES

19. KEY WORDS (Continue on reverse side if necessary and identify by block number)

Radar scattering
Intermittent contacts
Loaded scatterers
Target identification

20. ABSTRACT (Continue on reverse side if necessary and identify by block number)

The rapid discontinuous fluctuations observed in the scattering from a moving multielement target, known as the intermittent-contact RADAM effect, are produced by variations in the surface currents caused by motion-induced changes in current paths between the target elements. Such a target can be modeled as a loaded scatterer. Tracked vehicles produce very strong and distinctive RADAM modulation at VHF frequencies. The results of experimental studies using a 5:1 scale-model tank suggest that the principal source of the above effect in this type of vehicle is the contact between the drive sprocket and the track. Time-domain processing of

DD FORM 1 JAN 73 1473

EDITION OF 1 NOV 65 IS OBSOLETE

UNCLASSIFIED

SECURITY CLASSIFICATION OF THIS PAGE (When Data Entered)

19. KEY WORDS (Continued)

20 ABSTRACT (Continued)

the detected amplitude modulation can be used to develop RADAM signatures for tracked vehicles and to identify them in real time.